

Title: The neuroprotective effect of ethanol intoxication in TBI is associated with the suppression of ErbB signaling in PV-positive interneurons

Authors: Akila Chandrasekar¹ MSc, Florian olde Heuvel¹ MSc, Martin Wepler² MD, Rida Rehman MSc¹, Annette Palmer³ PhD, Alberto Catanese⁴ MSc, Birgit Linkus¹ Dipl.Ing PhD, Albert Ludolph¹ MD PhD, Tobias Boeckers⁴ MD PhD, Markus Huber-Lang³ MD PhD, Peter Radermacher² MD, Francesco Roselli^{1,4} MD PhD

Affiliation:

1. Dept. of Neurology, Ulm University
2. Institute of Anesthesiological Pathophysiology and Process Engineering- Ulm University
3. Institute of Clinical and Experimental Trauma-Immunology, Ulm University
4. Dept. of Anatomy and Cell Biology, Ulm University

Running title: ErbB in PV neurons mediates ethanol effect in TBI

Table of Contents title: Ethanol suppresses TBI-induced ErbB signaling in PV interneurons

Corresponding author: PD Francesco Roselli, MD, PhD

Dept. of Neurology-Ulm University

Center for Biomedical Research (ZBF)

Helmholtzstrasse 8/2(R1.44)-89081 Ulm-DE

Phone: 0049 0731 500 63147

Fax: 0049 0731 500 46111

Email: francesco.roselli@uni-ulm.de

Full author and contact information:

Akila Chandrasekar (graduate student): Dept. of Neurology-Ulm University

Center for Biomedical Research (ZBF)

Helmholtzstrasse 8/2-89081 Ulm-DE

Phone: 0049 0731 500 63147

Fax: 0049 0731 500 46111

Email: akila.chandrasekar@uni-ulm.de

Florian olde Heuvel (staff scientist): Dept. of Neurology-Ulm University

Center for Biomedical Research (ZBF)

Helmholtzstrasse 8/2-89081 Ulm-DE

Phone: 0049 0731 500 63149

Fax: 0049 0731 500 46111

Email: florian.oldeheuvel@gmail.com

Martin Wepler (postdoctoral fellow): Institute of Anesthesiological Pathophysiology
and Process Engineering-University Hospital,
Ulm

Center for Biomedical Research (ZBF)

Helmholtzstrasse 8/1-89081 Ulm-DE

Phone: 0049 0731 500 60161

Fax: 0049 0731 500 60162

Email: martin.wepler@uni-ulm.de

Rida Rehman (graduate student) Dept. of Neurology-Ulm University

Center for Biomedical Research (ZBF)

Helmholtzstrasse 8/2-89081 Ulm-DE

Phone: 0049 0731 500 63147

Fax: 0049 0731 500 46111

Email: rida.rehman@uni-ulm.de

Annette Palmer (postdoctoral fellow):

Institute of Clinical and Experimental Trauma-
Immunology

Center for Biomedical Research (ZBF)

Helmholtzstrasse 8/2-89081 Ulm-DE

Phone: 0049 0731 500 54810

Fax: 0049 0731 500 46111

Email: annette.palmer@uniklinik-ulm.de

Alberto Catanese (graduate student):

Dept. of Anatomy and Cell Biology

Albert-Einstein Allee 11-89081 Ulm-DE

Phone: 0049 0731 500 23213

Fax: 0049 0731 500 23217

Email: tobias.boeckers@uni-ulm.de

Birgit Linkus (staff scientist):

Dept. of Neurology-Ulm University

Center for Biomedical Research (ZBF)

Helmholtzstrasse 8/2-89081 Ulm-DE

Phone: 0049 0731 500 63057

Fax: 0049 0731 177 1202

Email: birgit.linkus@uni-ulm.de

Albert Ludolph (full professor):

Dept. of Neurology-Ulm University

Oberer Eselsberg 45-89081 Ulm-DE

Phone: 0049 0731 177 1200

Fax: 0049 0731 177 1202

Email: albert.ludolph@rku.de

Tobias Boeckers (full professor):

Dept. of Anatomy and Cell Biology

Albert-Einstein Allee 11-89081 Ulm-DE

Phone: 0049 0731 500 23221

Fax: 0049 0731 500 23217

Email: tobias.boeckers@uni-ulm.de

Markus Huber-Lang (full professor):

Institute of Clinical and Experimental Trauma-
Immunology

Center for Biomedical Research

Helmholtzstrasse 8/1-89081 Ulm-DE

Phone: 0049 731 500 54716

Fax: 0049 731 500 54718

Email: markus.huber-lang@uniklinik-ulm.de

Peter Radermacher (full professor):

Institute of Anesthesiological Pathophysiology
and Process Engineering-University Hospital,
Ulm

Center for Biomedical Research (ZBF)

Helmholtzstrasse 8/1-89081 Ulm-DE

Phone: 0049 0731 500 60161

Fax: 0049 0731 500 60162

Email: peter.radermacher@uni-ulm.de

Abstract:

Ethanol intoxication (EI) is a frequent comorbidity of TBI, but the impact of EI on TBI pathogenic cascades and prognosis is unclear. Although clinical evidence suggests that EI may have neuroprotective effects, experimental support is, to date, inconclusive. We aimed at elucidating the impact of EI on TBI-associated neurological deficits, signaling pathways and pathogenic cascades in order to identify new modifiers of TBI pathophysiology. We have shown that ethanol administration (5g/Kg) before trauma enhances behavioral recovery in a weight-drop TBI model. Neuronal survival in the injured somatosensory cortex was also enhanced by EI. We have used phospho- Receptor Tyrosine Kinase (RTK) arrays to screen the impact of ethanol on the TBI-induced activation of RTK in somatosensory cortex, identifying ErbB2/ErbB3 among the RTK activated by TBI and suppressed by ethanol. Phosphorylation of ErbB2/3/4 RTKs were upregulated in vGlut2+ excitatory synapses in the injured cortex, including excitatory synapses located on parvalbumin (PV)-positive interneurons. The administration of selective ErbB inhibitors was able recapitulate, to a significant extent, the neuroprotective effects of ethanol both in sensorimotor performance and structural integrity. Furthermore, suppression of PV interneurons in somatosensory cortex before TBI, by engineered receptors with orthogonal pharmacology, could mimic the beneficial effects of ErbB inhibitors. Thus, we have shown that EI interferes with TBI-induced pathogenic cascades at multiple levels, with one prominent pathway, involving ErbB-dependent modulation of PV interneurons.

Key words: Traumatic brain injury, ethanol intoxication, tyrosine kinase receptors, inhibitory interneurons, chemogenetics

Introduction

Brain trauma is a frequent cause of injury in civilian and military populations, with 577/100.000 cases per year reported in the US (between 2002 and 2006,) and even larger numbers in the developing world.^{1,2} Moderate-to-severe TBI accounts for 10-30% of the overall incidence but results, nevertheless, in 17.6/100.000 deaths per year in the United States alone.^{1,3} It is also estimated that 3.2-5.3 million patients live with long-term disability related to TBI in the United States.⁴ The overall survival in cases of severe TBI has changed very little in the last 20-30 years.⁵ Epidemiological evidence can be used to identify modifiers and modulators of TBI prognosis in humans, alleviating the pitfalls of target identification in rodent models.

Clinical data have shown that Ethanol Intoxication (EI) is a potential modifier of TBI outcome. EI is detected in up to 55% patients admitted for TBI with the great majority of patients displaying a binge-drinking pattern (i.e., not being chronic alcoholics).^{3,6} Surprisingly, positive Blood Alcohol Level (BAL) has been associated with a better outcome of TBI⁷⁻¹² although not in all studies.^{13,14} In particular, Berry *et al.* reported BAL >230mg/dL being strongly associated with reduced mortality in moderate-to-severe TBI.¹⁰ Likewise, patients with positive BAL showed a faster recovery of neurocognitive functions¹⁵, although other studies found detrimental or no effect.^{16,17}

The interaction between EI and TBI has been investigated in experimental models employing different TBI models and different schedules of ethanol administration: ethanol administration before a fluid-percussion injury¹⁸ or three-dose ethanol administration before and after controlled-cortical impact (in rats)¹⁹ worsened sensorimotor recovery, whereas single-dose ethanol administration soon after blunt TBI,¹² or before blunt TBI,²⁰ contusive TBI²¹ or controlled-cortical injury²² lead to faster recovery. Thus, EI may provide context-dependent beneficial effects in TBI, offering an entry point to understanding board or subtype-specific targets of intervention.

Mechanistic understanding of EI influence on TBI is limited: EI at the instance of trauma modulates the neuro-inflammatory cascade reducing the production of pro-inflammatory cytokines and enhancing the secretion of IL-13,^{20,23} although it is also reported to increase

brain edema.²⁴ Nevertheless, EtOH pharmacological spectrum of activities include antagonistic effects on NMDAR²⁵ and agonistic effects on GABAR,²⁶ suggesting that EI may affect multiple, distinct sets of biological functions in neurons, astrocytes and immune cells (such as synaptic plasticity, proliferation and inflammation) at once.

At molecular level, these functions are mediated and orchestrated (although not exclusively) by a set of Receptor Tyrosine Kinases (RTK) including, among many, the ErbB family and Trk family receptors (involved in synaptic plasticity and astrocyte proliferation),²⁷⁻²⁹ Axl/Dtk/Metk receptors (affecting microglia physiology),³⁰ EphA and EphB family receptors (modulating astrocyte responses).³¹ Since distinct sets of RTK control different biological responses and structures (synaptic plasticity, astroglial responses, neurovascular unit),^{28,31-34} monitoring the activation status of such receptors make it possible to probe the ongoing cellular responses elicited by TBI and the combination of EI and TBI. In particular, activation of the ErbB family RTK provides an entry point to the excitation/inhibition balance in the affected cortex: in fact, ErbB family members are expressed on inhibitory interneurons³⁵⁻³⁷ where they control the strength of excitatory synapses.^{27,38} Among the inhibitory interneurons, ErbB receptors are prominent regulators of Parvalbumin-positive (PV) Interneurons^{39,40} and thus provide an entry-point to the effects of EI and TBI on perisomatic inhibition and cortical excitability.⁴¹

Therefore, we monitored the impact of EI on behavioural and histological consequences of TBI and exploited an array of antibodies directed against phosphorylated RTK to identify the pattern of RTK activation in TBI and how this was influenced by EI. Because of the highly dynamic nature of phosphorylation events, this approach provided a more direct sampling of the ongoing signaling compared to gene-transcription profiling. In addition, since RTK are targeted by a growing number of small-molecules approved for human use (e.g.,⁴²), they provide opportunities for drug repurposing in TBI.

We have demonstrated that EI accelerates neurological recovery and ameliorates the histological damage caused by TBI. The RTK array analysis revealed that EI prevented the TBI-induced phosphorylation of several RTK and in particular the ErbB family. We have demonstrated that phosphorylated ErbB family members are localized in vGlut2 synapses

on inhibitory neurons and that neuroprotective effects of EI can be partially recapitulated by pharmacological modulation of ErbB or by chemogenetic control of parvalbumin interneurons.

Materials and Methods

Animals, Ethanol administration and Traumatic Brain Injury Model

The experiments described were approved by the local veterinary and animal experimentation service under the license n.1222 and successive integration. B6 mice were bred locally (Ulm University) under standard husbandry conditions (24°C, 60-80% humidity, 14/10 light/dark cycle, with ad libitum access to food and water). B6/PV-Cre mice were a kind gift of Pico Caroni (FMI, Basel) and were bred locally (Ulm University) under the same conditions. Experimental data are reported from a total of 194 mice from an overall cohort of 224 mice (with 30 mice experiencing acute mortality or meeting termination criteria, see below). Experimental groups and mice allocations for each group are summarized in supplementary table 1. For behavioural and histological analysis of EI/TBI interactions, the experimental design included four groups: i) control mice administered with saline and subject to sham surgery (sal-S; n=3); ii) control mice administered with high-dose ethanol (5g/kg) diluted in saline and subject to sham surgery (eth-S; n=3); iii) mice pretreated with saline before TBI (sal-TBI; n=8); iv) mice pretreated with high-dose ethanol (5g/kg) diluted in saline before TBI (eth-TBI; n=6). Ethanol solution (400µl of ethanol solution, 5g/kg in 32% v/v in saline or saline alone), diluted in saline was administered by oral gavage 30 min before the procedure.⁴³ WT male mice aged 80-90 days were subject to closed weight-drop TBI after administration of buprenorphine (0.1mg/kg by subcutaneously injection) and put under sevoflurane anesthesia (2,5% in 97,5% O₂). The scalp skin was incised on the midline to expose the skull. Animals were then manually positioned in the weight-drop apparatus as previously described with the impactor site localized at the center of the right parietal bone. TBI was delivered by a 333g impactor free-falling from a 2cm distance.⁴³ Immediately after the experimental TBI, animals were administered 100% O₂ and were monitored for the apnea time. After spontaneous breathing was restored, the scalp skin of the anesthetized mice was stitched

with Prolene 6.0 surgical thread and the animals were transferred to a warmed recovery cage (single-housed) with ad libitum access to food and water. Additional doses of buprenorphine were administered every 12h for the following 24h post-injury. For sham-surgery, mice were subject to the same procedures and treatments (anesthesia, skin opening and closure, handling, positioning in the TBI apparatus) but no trauma was delivered.

To avoid unnecessary suffering of the mice, their general state was checked regularly using a score sheet developed for TBI determining fixed termination criteria. Effort was made to minimize animal suffering and reduce the number of necessary animals.

Phospho-RTK Screening:

For the screening of RTK activation pattern, a single time-point (3h) was considered and four experimental groups were included: i) saline-sham (n=8), ii) ethanol-sham (n=5), iii) saline-TBI (n=7) and iv) ethanol-TBI (n=5). Mice were sacrificed 3h after TBI (or sham surgery) by cervical dislocation and the brain was quickly dissected in ice-cold PBS. Cortex samples 1.5-2 mm in diameter were dissected from the parietal lobe (somatosensory area) and snap frozen. In order to obtain cortical protein extracts, cortical samples were thawed in homogenization buffer (1X Lysis Buffer; CST; 20mM Tris-HCl (pH 7.5), 150mM NaCl, 1mM Na₂EDTA, 1mM EGTA, 1% Triton, 2.5mM sodium pyrophosphate, 1mM β -glycerophosphate, 1mM Na₃VO₄, 1 μ g/ml leupeptin) containing Phosphatase (1 tablet per 10ml lysis buffer) and Protease (1 tablet per 50ml lysis buffer) inhibitor (Roche cOmplete tablets, Sigma-Aldrich, Taufkirchen, Germany) cocktail and homogenized with 20 strokes of Dounce apparatus. Tissue homogenates were then cleared by centrifugation (10.000g, 10min) and assayed for protein concentration with the Bradford Protein Assay.

Phospho-RTK activation screening was based on a nitrocellulose-membrane sandwich immunoassay and was performed according to the manufacturer's instructions (R&D Systems, Minneapolis). Briefly, nitrocellulose membrane spotted with the anti-RTK antibody were blocked in Array buffer 1 for 1h at RT, before being incubated with 500 μ g of tissue homogenates diluted in 1.5mL of Array buffer 1 for 24h at 4°C. Thereafter, membranes were quickly rinsed in sterile water and washed 3 x 10 min in Wash Buffer.

Membranes were then incubated with the Anti-Phospho-Tyrosine-HRP Detection Antibody, diluted to 1X Array Buffer 2, for 2h at RT. Membranes were then washed again as before and detection of the HRP was performed by adding to each membrane 1mL of the Chemi Reagent Mix and imaged using the chemiDOC MP Imaging System from Bio Rad.

Array images were then quantified using ImageJ. A fixed-size ROI was drawn on each antibody spot and the integrated median gray value was obtained, together with a value for the local background. Each experimental run contained at least two saline-sham samples, and values for each spot were expressed as percentage of the saline-sham reference.

Drugs and Drug Administration

The ErbB2 inhibitor Lapatinib (Selleck chemicals, Munich, Germany), the ErbB inhibitor AG825 (Tocris, Bristol, UK), the broad-spectrum TK inhibitor LDN-211904 (Merck, Darmstadt, Germany) and the PDGF inhibitor CP-673451 (Selleck Chemicals, Munich, Germany) were commercially available. Each drug was dissolved in a minimal volume of DMSO and diluted in vehicle (containing 5%PEG-400, 5%Tween-80, 90% saline) before administration. Mice were administered with each drug in a volume of 400µl of vehicle by oral gavage. The experimental design included i) mice administered with vehicle undergoing sham-surgery (veh-S; n=4), ii) mice pretreated with ethanol (5g/kg) diluted in vehicle and undergoing sham surgery (eth-S; n=3), iii) mice administered with vehicle undergoing TBI (veh-TBI; n=5), iv) mice pretreated with ethanol and undergoing TBI (eth-TBI; n=4) and v) mice pre-treated with specific inhibitors undergoing TBI. For ErbB inhibitors Lapatinib and AG825, two treatment doses were considered, 10mg/kg (n=6 and n=5, respectively) and 50mg/kg (n=4 and n=4, respectively). For LDN-211904 (n=4) and CP-673451 (n=4) only one dose (10mg/kg) was considered. In the pre-treated mice, all drugs (or vehicle alone) were administered 30 min before TBI. In addition to the four groups cited above, for Lapatinib and AG825 one more group was analyzed, vii) mice treated with the specific inhibitor 30min after TBI (n=4 and n=4, respectively). In this group, only one dose (50mg/kg) was administered. Of note, administration of ethanol diluted in saline or

saline alone did not produce a significantly different effect on behavioral or histological readouts than ethanol diluted in PEG400-Tween80-saline vehicle or of vehicle alone.

Behavioural and Neurological Score assessment:

The overall neurological impairment was evaluated using the composite Neurological Severity Score, as described by Flierl et al.⁴³ At 3h post-injury, 24h post-injury, 2dpi, 3dpi, 5dpi and 7dpi the assessment of motor (muscle status, abnormal movement), sensory (visual, tactile, proprioceptive), reflex, and balance abilities were tested. Animals are awarded one point for failure to perform a task, such that scores ranged from 0 to 10, increasing with the severity of dysfunction. The Arena Escape test, part of NSS evaluation, was performed putting the animals into a circular, brightly-lit area whose wall included a narrow opening leading to the dark compartment. The time required to enter the dark compartment was measured and averaged over three attempts. The Beam walk test was performed as previously reported: mice were habituated to walking over a suspended wooden beam, from an open platform to a dark compartment and the test was then repeated at 2dpi and 7dpi.⁴⁴ The time required to reach the dark box was measured.

Immunostaining, confocal imaging and image analysis:

For the evaluation of ErbB family members phosphorylation by immunostaining, mice treated with either i) saline (sal-S; n=3) or ii) ethanol (eth-S; n=3) were subject to sham surgery, and independent groups of iii) saline-pretreated (sal-TBI; n=5) and iv) ethanol-pretreated (eth-TBI; n=4) mice underwent the TBI procedure (as indicated above). In order to further evaluate the phosphorylation of ErbB2 after the administration of ErbB specific inhibitors: AG825 and Lapatinib, the following groups were considered: i) mice treated with vehicle and undergoing sham surgery (veh-S, n=3), ii) mice treated with vehicle and undergoing TBI (veh-TBI, n=3), iii) mice treated with AG825 inhibitor and undergoing TBI (n=3) and iv) mice treated with Lapatinib and undergoing TBI (n=3). Mice were perfusion-fixed (25 ml ice-cold PBS followed by 50ml of ice-cold 4% PFA in PBS) after 3h or 7 days. Brains were dissected and stored in PFA (4% in PBS) for 18h at 4°C, before being washed in PBS, cryoprotected in 30% sucrose in PBS and embedded in OCT (TissueTek, Sakura). Sections were cut in cryostat at 40µm thickness. Immunostaining was performed as

previously reported.⁴⁶ Briefly, free-floating brain sections spanning the trauma site were blocked in BSA 3%+Donkey serum 3%+Triton 0.3% in PBS for 2h at 24°C and incubated with primary antibody in blocking buffer for 40h at 4°C. The following primary antibodies were used: rabbit anti phosphorylated-ErbB2 (pErbB2, 1:200, CST, #2243), rabbit anti phosphorylated-ErbB3 (pErbB3, 1:1000, CST, #2842), phosphorylated ErbB4 (pErbB4 1:400, Abcam, ab109273), mouse anti vGlut1 (1:500, Synaptic System, #135311), guinea pig anti vGlut2 (1:500, Synaptic System, #135404), mouse anti Synaptotagmin-2 (1:200, abcam, ab154035), goat anti Parvalbumin (1:1000, Swant, PVG-214). For the detection of phospho-ErbB2 and phospho-ErbB3 and phospho-ErbB4, the tyramide signal amplification protocol was used (Alexafluor-488 Tyramide SuperBoost kit, Thermo Fisher Scientific, B40922) and the manufacturer's instructions were modified according to free floating staining. Briefly, the sections were washed 3x10 min in PBS at room temperature and incubated for 60 min with poly-HRP-conjugated secondary antibody. After washing (3x30min in PBS at room temperature), the sections were incubated in tyramide working solution (100X tyramide stock solution, 100X H₂O₂ solution and 1X reaction buffer) for 10min, the tyramide working solution was stopped by adding the sections in stop reagent. After washing (3x30min in PBS at room temperature), brain sections were incubated with opportune secondary antibodies (Alexa-conjugated donkey anti-mouse, anti-rabbit, anti-guinea pig) diluted 1:500 together with the nuclear stain TOPRO-3 (Invitrogen) 1:1000 for 2h at room temperature and mounted using FluoroGold mounting medium. For the assessment of neuronal loss, the following groups were considered: i) mice administered with vehicle and undergoing sham surgery (veh-S; n=3), ii) mice administered with ethanol (eth-S; n=3, 5g/kg, diluted in vehicle) undergoing sham surgery, iii) mice administered with vehicle undergoing TBI (veh-TBI; n=5), iv) mice administered with ethanol undergoing TBI (eth-TBI; n=4), v) mice administered with AG825 or Lapatinib (n=5 and n=6, respectively) and vi) mice administered with LDN or CP (n=4 and n=4, respectively). Mice were sacrificed at 7 dpi by perfusion/fixation and the brain tissue was then processed for immunostaining as reported above. Immunostaining was performed with mouse anti neuN (1:100, Millipore, MAB377) with the same experimental protocol detailed above.

Confocal images were acquired using an LSM-700 (Carl Zeiss AG) inverted microscope, fitted with a 20x air or 40x oil objective. All images were acquired in 12-bit format and imaging parameters were set in order to obtain signal for the immunostained antigen >150 while avoiding saturation in high-intensity neurons. For neuronal density measurements, regions of interest corresponding to the trauma site and spanning the surrounding regions for at least 1500 μ m were acquired with 20x objective in tile-scan mode, with optical section thickness set at 1 μ m. Neuronal nuclei were counted in ROI located in the primary injury site (on the axis of the injury site; supplementary figure 1) and in the penumbral zone (located at a fixed distance of 400 μ m from the axis of the injury site; supplementary figure 1). Multiple brain sections spanning the injury site were imaged and the ones with the largest extent of injury (measured in the latero-lateral axis) were considered as reference for the evaluation of the injury size.

For phospho-RTK quantification, images were acquired with 40x objective with optical thickness set at 500nm and using the tile-scan mode to acquire composite pictures spanning the primary injury site and the penumbra. Confocal image stacks composed of 10 optical sections were collapsed in maximum-intensity projection using the imageJ software suite. For overall pErbB2, pErbB3 and pErbB4 levels, two fixed-size rectangular ROI were located symmetrically on each side of the axis of the injury site and the mean gray value was computed.

For the analysis of pErbB2 colocalization with synaptic markers, single optical sections acquired with the 40x/oil objective were considered and each channel was acquired independently to prevent fluorescence cross-bleed. Each synaptic marker was evaluated independently against pErbB2 (the following co-immunostaining were performed pErbB2/vGlut1, pErbB2/vGlut2, and pErbB2/Syt2). Multi-channel images were processed in ImageJ; ROI for synaptic analysis were located at 40-50 μ m from the axis of the injury site. pErbB2 fluorescence images from veh-TBI samples were thresholded to allow a binary classification and the co-localization of pErbB2+ synapses and vGlut1, vGlut2 or Synaptotagmin was visually evaluated by listing the number of pErbB+ synapses also displaying >10 pixels positive for each synaptic marker considered. A minimum of 150 synapses for each marker were evaluated (from 3 replicates) and the percentage of

pErbB2+/vGlut1+, pErbB2+/vGlut2+ and pErbB2+/Synt2+ synapses (over the total number of pErbB2+ in the considered ROI) was computed.

Intracerebral Injection of AAV and Chemogenetic Agonist Administration:

For the study of PV activation or inhibition by chemogenetics, and the eventual additive effect of ethanol, PV-Cre mice were injected with AAV9 expressing either activator PSAM or inhibitor PSAM. For both the former and the latter (independently), the following experimental design was considered: i) mice injected with saline and subject to sham surgery (sal-actPSAM-S and sal-inhPSAM-S, both n=3), ii) mice injected with PSEM and subject to sham surgery (PSEM-actPSAM-S and PSEM-inhPSAM-S, both n=3), iii) mice injected with saline and subject to TBI (sal-actPSAM-TBI and sal-inhPSAM-TBI, both n=4), iv) mice injected with PSEM and subject to TBI (PSEM-actPSAM-TBI and PSEM-inhPSAM-TBI, both n=5), v) mice injected with PSEM, administered ethanol and subject to TBI (eth-PSEM-actPSAM-TBI and eth-PSEM-inhPSAM-TBI, both n=4) and vi) mice administered with ethanol alone and subject to TBI (eth-actPSAM-TBI and eth-inhPSAM-TBI, both n=3). Intracerebral injection of AAV vector was performed at the age of P30-P40 as previously reported.⁴⁷ Briefly, mice were pretreated with buprenorphine (0.01 mg/Kg; Reckitt Beckiser Healthcare, Berkshire, UK) and meloxicam (1.0 mg/Kg; Böhringer Ingelheim, Biberach an der Riß, Germany) before being put into a stereotaxic frame (Bilaney Consultants GmbH D-40211 Düsseldorf, Germany) under continuous isoflurane anesthesia (4% in O₂ at 800 ml/min). Skin scalp was incised on the midline to expose the skull. Using a hand-held micro drill, a burr hole was drilled at the coordinates (x=+2.0, y=-2.0), corresponding to the primary somatosensory cortex. AAV9 vectors, encoding floxed PSAM-carrying AAV9 (excitation, pAAV(9)-pCAG-flox-PSAM(Leu41Phe,Tyr116Phe)5HT3-WPRE; inhibition, pAAV(9)-cbaflox-PSAM(Leu141Phe,Tyr116Phe)GlyR-WPRE) was obtained from Vector Biolabs (Malvern-PA, US) at the titre of 9*10⁹ viral genomes/ml. 200-500nl of viral suspension were injected at z=-0.4/0.7 using a pulled-glass capillary connected to a Picospritzer microfluidic device. Injection was performed with 10msec pulses over 10min and the capillary was kept in place for 10 more minutes before being withdrawn.^{13, 48} Scalp skin was stitched with Prolene 7.0 surgical threads and animals were transferred for recovery in single cages with facilitated access to water and food. Animals were monitored

for eventual neurological impairment for the following 72h and were administered additional doses of buprenorphine if needed. TBI procedure was performed 30-40days after viral injection. No increase in mortality or morbidity was observed in mice intracranially-injected in comparison to mice which were subject to TBI but were never subject to microdrilling and viral injection (corresponding to the saline-TBI or vehicle-TBI mice used as controls in behavioural and pharmacological experiments). The PSEM308 agonist (obtained from Apex Scientific Inc. Stony Brook-NY, US)⁴⁸ was administered as previously reported⁴⁷ at the dose of 5g/Kg 20-30 min before the TBI procedure by intraperitoneal injection (diluted in sterile saline at 20 mg/ml). The administration of ethanol was performed as reported above (oral gavage, diluted in saline, 5g/kg).

Blood Gas Analysis:

For the evaluation of hypoxemia and hypercapnia which may result from the interaction of ethanol intoxication and TBI, blood gas analysis was performed. Three experimental groups were considered i) ethanol administered, sham TBI (n=3) ii) saline-pretreated and TBI (n=3) iii) ethanol-pretreated, TBI (n=4). Baseline reference values for PaO₂ and PaCO₂ were obtained from Schwarzkopf et al., 2013.⁴⁹ Briefly, 50µl of arterial blood was drawn from the abdominal aorta in calcium-heparin-containing syringes. Blood gas tensions were measured using a Radiometer ABL 800® blood gas analyzer.

Blood GFAP Assay:

For GFAP blood measurements, the following experimental groups were considered: i) mice administered with saline undergoing sham surgery (n=3), ii) mice administered with ethanol (5g/kg) and undergoing sham surgery (n=3), iii) mice administered with saline undergoing TBI (n=4) and iv) mice administered ethanol undergoing TBI (n=4). Whole blood was taken by puncture of the right ventricle und transferred into sterile plasma EDTA microtubes (Kabe Labortechnik, Nuembrecht-Elsenroth, Germany). After centrifugation at 800g for 10min at 4°C, the supernatant was taken and centrifuged at 13000g for 2min at 4°C. Plasma samples were analyzed by commercially-available enzyme-linked immunosorbent assay (ELISA) specified for mouse GFAP, according to the manufacturer's instructions (LSBio, Seattle, USA). Colorimetric detection was made at a

wavelength of 450nm using a plate reader (Tecan Sunrise Plate Reader, Tecan, Crailsheim, Germany).

Blood Ethanol Assay:

For the assessment of blood Ethanol levels, we considered the following groups for both the 15 min and the 3h time point (two independent cohorts of mice for each time point): i) saline-Sham (sal-S; n=3), ii) ethanol-Sham (eth-S; n=3), iii) saline-TBI (sal-TBI; n=4) and iv) ethanol-TBI (eth-TBI; n=4). Blood ethanol analysis was performed on blood plasma taken from mice after TBI with or without Ethanol administration. The analysis was performed using the manufacturer's instructions (Abcam plc, Cambridge, UK). Briefly, plasma (obtained as for the GFAP assay) was diluted 1:500 for ethanol treated samples and 1:10 for saline treated samples. The standard was used at 0.1mM pure Ethanol Standard in Ethanol Assay Buffer. 50µl of diluted sample was added to each well and 50µl of reaction mix (46µl Ethanol Assay buffer, 2µl Ethanol Probe and 2µl Ethanol Enzyme Mix) was added. The wells were shortly mixed, incubated for 30min at room temperature and the output was measured with OD 570 (Fluostar Optima plate scanner, BMG LABTECH).

Statistics

Statistical analysis was performed using the GraphPad Prism software suite. The analysis of behavioural performance and the RTK arrays was done using two-way ANOVA, with Tuckey post-hoc test. For the comparison of neuronal density values, one-way ANOVA with Bonferroni correction for multiple comparisons was applied. For the comparison of blood GFAP levels and blood ethanol levels, since the data distribution did not approximate a normal distribution, non-parametric Mann-Whitney test was used. Behavioural data are displayed as mean±SEM. Statistical significance was set at p<0.05. Statistical significance has been reported in figures as follows: **** = p<0.0001; *** = p<0.001 ; ** p<0.01; * = p<0.05

Results

Acute Ethanol Administration accelerates neurological recovery after TBI

To establish the effect of ethanol on the behavioral and sensorimotor outcome of TBI, we administered a single dose of ethanol (5g/kg or saline) by oral gavage 30min before mice were subjected to experimental TBI (or sham surgery). All mice undergoing TBI displayed a brief apnea time, whose duration was comparable in the ethanol-treated groups and in saline-treated mice ($6.3\pm 1.0s$, $6.8\pm 1.1s$ vs $7.1\pm 1.4s$, respectively; $p>0.05$). We monitored the progression of neurological deficits using the NSS score and two sensorimotor tests, the Beam Walk and the Arena Escape Test.

The NSS score displayed a significant effect of TBI ($F_{(3,11)}=39.7$, $p<0.0001$), of time ($F_{(5,55)}=29.8$, $p<0.0001$) and a significant TBI x time interaction ($F_{(15,55)}=10.1$, $p<0.0001$). Post-hoc analysis revealed at 3h, a significant difference post injury with the TBI groups having a significantly higher NSS score than sal-S or eth-S mice (0.5 ± 0.5 and 0.5 ± 0.5 , respectively), although there was no difference in the NSS scores among sal-TBI and eth-TBI mice (5.0 ± 1.5 in sal-TBI vs 3.5 ± 1.5 in eth-TBI, $p=0.12$; figure 1A). Both sal-TBI and eth-TBI mice displayed a progressive recovery in NSS score, however, the eth-TBI displayed a trend toward faster neurological recovery (at 24h post injury, NSS was 3.5 ± 1.5 and 2 ± 1.0 for sal-TBI and eth-TBI, respectively; $p=0.067$; at 2dpi, NSS was 2.0 ± 1.0 and 1.5 ± 0.5 in sal-TBI and eth-TBI, respectively; $p=0.55$; figure 1A).

Latency to escape a brightly-lit arena via a small slit (arena escape test, AE) was significantly affected by TBI (TBI on AE: $F_{(3,20)}=6.5$, $p=0.003$). However, the effect of time on AE was not significant ($F_{(3,54)}=2.6$, $p=0.058$). Post-hoc analysis revealed that escape time was longer in sal-TBI than in sal-S mice (at 2dpi, $15.8\pm 6.1s$ vs $5.3\pm 2.4s$, $p=0.0036$), whereas eth-TBI mice ($6.4\pm 2.2s$) performed significantly better than sal-TBI (eth-TBI vs sal-TBI $p=0.045$; eth-TBI vs eth-S $p=0.75$; figure 1B). Notably, the performance of sal-TBI mice did not improve over time (at 7 dpi $12.7\pm 4.6s$; $p<0.001$ sal-TBI vs sal-S) and the performance of eth-TBI mice stayed at control (eth-S and sal-S) level.

When sensorimotor skills were tested in the 11mm round beam walk (BW) test, a significant effect of TBI on BW was detected ($F_{(3,18)}=15.2$, $p<0.0001$) and of time on BW

($F_{(3,54)}=21.7$, $p<0.0001$), with a significant interaction between TBI and time ($F_{(9,54)}=3.4$, $p=0.0021$). Post-hoc analysis revealed that sal-TBI mice performed significantly worse than sham controls (at 2dpi time point, 29.3 ± 6.8 s in sal-TBI as compared to 7.9 ± 1.6 s in sal-S; $p<0.0001$; figure 1C) although the performance recovered over time (at 7 dpi, 12.6 ± 2.2 s vs 7.8 ± 1.9 s; $p=0.682$). However, eth-TBI mice performed significantly better than saline-pretreated ones after TBI (at 2dpi, 17.8 ± 5.8 s vs 29.3 ± 6.8 s, respectively; $p<0.0001$) and recovered to baseline level in shorter time (at 3 dpi 18.6 ± 3.4 s in sal-TBI as compared to 9.1 ± 1.8 s in eth-TBI and 7.6 ± 1.2 s in eth-S; eth-TBI vs eth-S $p=0.78$; sal-TBI vs sal-S $p<0.001$). Sal-S and eth-S were always identical in their performance (figure 1C).

The observed differences in the beam walk and in the arena escape tests were not due to an overall impairment in locomotion. In fact, when tested in the open field, the average speed was not statistically different between sal-TBI and eth-TBI mice at 2dpi or at later time points (2dpi: 6.7 ± 3.2 cm/s, 7.7 ± 6.3 cm/s and 11.1 ± 6.0 cm/s for sham, sal-TBI or eth-TBI, respectively; 7dpi: 11.2 ± 7.9 cm/s, 7.0 ± 5.0 cm/s and 12.0 ± 6.2 cm/s for sham, sal-TBI or eth-TBI, respectively; two-ways ANOVA, time x treatment group, $p>0.05$).

In order to exclude possible respiration-depressing effects of ethanol after TBI, we measured PaO_2 and PaCO_2 on arterial blood in a dedicated cohort of mice, administered either saline or ethanol, which underwent TBI and were sacrificed 15min later. Despite the high dose, ethanol did not affect respiratory drive in addition to any putative anesthesia-induced respiratory depression: the measurement of arterial blood gas tensions immediately after TBI yielded PaCO_2 values 35 ± 7 mmHg ($n=3$) and 36 ± 13 mmHg ($n=4$; $p>0.05$) in the vehicle and ethanol-treated animals, respectively. This demonstrates that there was no major additional ethanol effects on respiratory drive and/or alveolar ventilation (likewise, in eth-Sham ($n=3$), PaCO_2 was comparable 36 ± 1 mmHg). Similarly, we excluded the occurrence of ethanol- or TBI-induced hypoxemia, since the blood gas analyses showed comparable immediate post-TBI PaO_2 values (282 ± 121 vs. 212 ± 79 mmHg, in the vehicle and ethanol-treated animals respectively as compared to 267 ± 47 mmHg in eth-S mice; $p>0.05$).

We also measured blood alcohol levels 15min and 3h (in two distinct cohort of mice) after trauma, to verify if ethanol levels are comparable in eth-S and eth-TBI. At the 15min time point, eth-S and eth-TBI displayed comparable levels of blood ethanol ($10.0 \pm 0.9 \mu\text{mol}$ and $14.6 \pm 2.7 \mu\text{mol}$, respectively; $p=0.057$; figure 1D). However, in mice sacrificed at the 3h time point, blood ethanol levels were significantly higher in eth-TBI mice than in eth-S ($2.7 \pm 1.4 \mu\text{mol}$ in eth-sham vs $10.0 \pm 1.2 \mu\text{mol}$ in eth-TBI, corresponding to $125 \pm 68 \text{mg/dL}$ and $461 \pm 56 \text{mg/dL}$, respectively; $p < 0.05$); negligible levels of ethanol were detected in saline-administered mice ($0.04 \pm 0.04 \mu\text{mol}$ and $0.03 \pm 0.03 \mu\text{mol}$ in sal-S and sal-TBI, respectively; figure 1D). In addition, we measured blood GFAP levels (a proxy of the severity of parenchymal damage caused by TBI in human and murine models) at the 3h time point: plasma GFAP was strongly elevated in both TBI groups compared to sham mice, but were not significantly affected by ethanol ($1.25 \pm 0.32 \text{ng/ml}$ in sal-TBI vs $1.17 \pm 0.42 \text{ng/ml}$ in eth-TBI, as compared to $0.058 \pm 0.004 \text{ng/ml}$ and $0.058 \pm 0.013 \text{ng/ml}$ in sal-S and eth-S groups, respectively; $p > 0.05$ for sal-TBI vs eth-TBI; figure 1E).^{29, 30}

Taken together, these data show that sensorimotor abilities were significantly conserved after trauma in ethanol-treated TBI mice compared with sal-TBI, suggesting an acute neuroprotective effect of ethanol.

Screening RTK activation identifies multiple signaling cascades activated by TBI and affected by ethanol

In order to gain mechanistic insights on the neuroprotective effect of EI in TBI, we set out to screen the phosphorylation level (in other words, the activation status) of 38 different receptor tyrosine kinases (RTK) representing multiple functional pathways (including neuronal, glial, vascular, inflammatory responses) and endowed with high translational potential. To achieve this aim, we sampled the trauma site from mice treated with saline or ethanol which underwent TBI or sham surgery. Whole-cortex protein extracts were then probed for RTK phosphorylation using nitrocellulose antibody arrays.

For 4 phospho-RTK (EphA7, EphA8, EphB2, EphB4) absolute levels were below the detection limit and could not be analyzed. Two-way ANOVA revealed a statistically significant difference between treatment groups ($F_{(3,21)} = 15.25$, $p < 0.0001$) and a significant

interaction between TBI and EI ($F_{(102,714)} = 3.005$, $p < 0.0001$). Post-hoc analysis (35 groups, 6 comparisons per group) revealed that Sal-TBI caused a statistically significant upregulation of the phosphorylation levels of 9 RTKs (ErbB2, $p = 0.011$; ErbB3, $p = 0.001$; FGFR1, $p = 0.0004$; FGFR3, $p = 0.0311$; HGF-R/c-Met, $p < 0.0001$; MSP-R, $p = 0.022$; EphA2, $p < 0.0001$; EphA3, $p < 0.0001$; EphA6, $p = 0.0204$) and the downregulation of 1 RTK (IGF-R1) when compared to sham samples which not reach statistical significance after multiple-comparisons correction.

Ethanol displayed a mainly negative effect on TBI-activated RTK, although not all activated RTK were equally downregulated by EI (figure 2A-B). When sal-TBI and eth-TBI groups were compared post-hoc, EI caused a statistically significant downregulation of 9 RTK: ErbB2 ($154 \pm 15\%$ in sal-TBI vs $73 \pm 26\%$ in eth-TBI; $p = 0.0003$), ErbB3 ($166 \pm 19\%$ in sal-TBI vs $67 \pm 20\%$ in eth-TBI; $p < 0.0001$), FGFR1 ($170 \pm 31\%$ in sal-TBI vs $75 \pm 21\%$ in eth-TBI; $p = 0.001$). Other RTK whose activation was significantly reduced by ethanol include PDGF-Rb ($138 \pm 16\%$ in sal-TBI vs $67 \pm 21\%$ in eth-TBI; $p = 0.0029$), Flt-3 ($135 \pm 49\%$ in sal-TBI vs $71 \pm 34\%$ in eth-TBI; $p = 0.0088$), EphA2 ($190 \pm 72\%$ in sal-TBI vs $137 \pm 51\%$ in eth-TBI; $p = 0.04$), MSP-R (150 ± 109 in sal-TBI vs $93 \pm 85\%$ in eth-TBI; $p = 0.0237$), EphA3 (although with large variations: $209 \pm 103\%$ in sal-TBI vs $152 \pm 33\%$ in eth-TBI, $p = 0.0243$) EphA6 and EphB1 (EphA6: $152 \pm 33\%$ in sal-TBI vs $75 \pm 19\%$ in eth-TBI, $p = 0.0011$; EphB1 $138 \pm 22\%$ in sal-TBI vs $64 \pm 11\%$ in eth-TBI, $p = 0.0041$). Additionally, some RTK were not affected by ethanol, such as HGFR/c-Met ($269 \pm 151\%$ in sal-TBI vs $255 \pm 121\%$ in eth-TBI; $p > 0.05$), FGFR3 ($147 \pm 35\%$ in sal-TBI vs $108 \pm 35\%$ in eth-TBI; $p > 0.05$).

Taken together, these data suggest that the effect of ethanol in TBI is multifaceted and involves the modulation of multiple signaling cascades unfolding in possibly multiple cellular subpopulations.

ErbB2, ErbB3 and ErbB4 phosphorylation is upregulated by TBI and it is downregulated by concomitant EI

Among the multiple RTKs modulated by TBI and ethanol, we decided to analyze in further detail the effect of TBI and ethanol intoxication on ErbB2/3/4 activation and signaling, because of their high expression in the cerebral cortex and because of their translational

value since these receptors can be targeted with FDA-approved small molecules.^{42,52,53}

First, we sought to validate the screening results and to identify the cellular sources of the phosphorylated RTKs by immunostaining of brain sections (sampling the trauma site) from sal-sham, eth-sham, sal-TBI or eth-TBI mice (perfused 3h after TBI) for phosphorylated ErbB2 (pY1221/1222), phosphorylated ErbB3 (pY1289) and phosphorylated ErbB4 (pY1284).

At 3h post injury, pErbB2, pErbB3 and pErbB4 immunofluorescence levels were strongly increased in the site of injury in sal-TBI mice compared to sal-sham control cortical samples and nearby cortices (371±68%, 422±73% and 321±57% of baseline, respectively; $p < 0.01$; figure 3A-F). Notably, while eth-sham did not display significantly lower levels of pErbB2, eth-TBI mice showed a significant reduction in pErbB2 fluorescence intensity (204±47% of sal-sham; $p < 0.05$ vs sal-sham and vs sal-TBI; figure 3A-B). Likewise, ethanol pretreatment resulted in the blunting of TBI-induced upregulation of pErbB3 and pErbB4 (249±51% and 203±48.9% of baseline, respectively; $p < 0.01$ sal-sham and vs sal-TBI; figure 3C-D and 3E-F). Thus, immunostaining data validated the antibody array findings and demonstrated the suppressive effects of ethanol on ErbB family activation after TBI.

pErbB2 and pErbB3 (and, to a lesser extent, pErbB4) displayed a strikingly punctuate pattern, reminiscent of synaptic localizations in the areas proximal to the injury site and in the penumbra. pErbB4 also displayed immunolocalization in cell bodies and proximal dendrites of a subset of neurons. In fact, when cortical samples were co-immunostained for pErbB2 together with the excitatory presynaptic markers vGlut1 and vGlut2, pErbB2 puncta colocalized almost exclusively with vGlut2⁺ puncta (93±4%) and very little with vGlut1 (3±2%) and never with the marker of inhibitory synapses, Synaptotagmin-2 (figure 3G-H).

Acute administration of ErbB2 inhibitors mimics ethanol effect on TBI behavioral outcome.

We further investigated the importance ethanol-induced suppression of RTK, particularly of ErbB- signaling in TBI. More accurately, we explored if specific RTK inhibitors could recapitulate EI-associated improved behavioural outcomes. Since the pharmacokinetics of ErbB inhibitors have not been studied in the context of TBI (Lapatinib penetration of the

brain has been previously assessed, although in a condition in which no CNS insult was delivered),⁵⁴ we verified that pre-administration of 50mg/kg of the ErbB inhibitors AG825 and Lapatinib (or vehicle) could affect pErbB2 levels in the cortex after TBI. Mice were sacrificed 3h after trauma and pErbB2 immunofluorescence levels were assessed: whereas in sal-TBI we detected a significant increase in ErbB2 phosphorylation in vGlut2⁺ synapses (Sal-TBI 354±60% vs sal-s; p<0.01 vs sham), TBI-induced pErbB2 increase was strongly limited by pretreatment with AG825 50mg/kg (AG825-TBI 162±46% vs sal-S; p<0.01 vs TBI; supplementary figure 2) or Lapatinib 50 mg/kg (Lapatinib-TBI 153±65% of sal-S; p<0.01 vs TBI; supplementary figure 2)

Thereafter, distinct groups of mice were administered ErbB2 inhibitors (AG825, 50mg/kg, or Lapatinib, 50mg/kg) a PDGFR inhibitor (CP-673451, 10mg/kg) or the broad RTK inhibitor (LDN-211904, 10mg/kg), in a single administration before TBI, and assessed for their performance in sensorimotor and behavioral tests. We also considered two groups of mice treated with a lower dose (10mg/kg) of either Lapatinib or AG825. For comparison, independent groups of mice were pretreated with ethanol diluted in vehicle or with vehicle alone and subject to sham surgery or to TBI. No difference in performance in any test was detected between veh-S and eth-S mice, which were comparable to saline-pretreated mice (cfr. Figure 1).

When assessed in the beam-walk test, mice treated with the 50mg/kg of AG825 or Lapatinib performed significantly better than vehicle-treated TBI mice and comparable to eth-TBI mice (at 2dpi, 10.1±2.7s and 12.6±2.4s, respectively, as compared to 30.9±7.8s in veh-TBI and 14.3±2.8s in eth-TBI mice; p<0.001 vs veh-TBI for both compounds; ethanol was diluted in vehicle for proper comparison; figure 4A). The effect of ErbB inhibitors was still detectable when a 10mg/kg dose was administered, with trends toward dose-dependent effects (although for AG825 the strong trend did not reach statistical significance; at 2dpi, 15.1±2.3s and 17.3±3.4s and; p=0.071 for AG825 10mg vs 50mg; p<0.05 for Lapatinib 10mg vs 50mg; figure 4A). The broad-selectivity RTK inhibitor LDN-211904 also produced a significant improvement in performance (8.6±3.4s; p<0.01 vs veh-TBI; figure 5A) whereas the PDGFR-selective drug CP-673451 did not affect significantly the performance (at 2dpi, 22.0±6.5s; p>0.05 vs veh-TBI; figure 4A). At 7dpi, eth-TBI as well as

mice treated with either dose of Lapatinib, AG825 or LDN were similar in performance to sal-S or eth-S mice, whereas sal-TBI were still significantly slower (figure 4B).

Likewise, performance in the arena escape test was significantly modified by RTK inhibitors. Both 10mg/kg and 50mg/kg AG825- and Lapatinib-treated mice performed significantly better than vehicle-treated ones after TBI (at 2dpi, $9.1 \pm 2.4s$ and $6.4 \pm 1.1s$ for AG825 and $11.3 \pm 1.3s$ and $7.5 \pm 1.6s$, respectively, vs $17.2 \pm 2.4s$, $p < 0.05$; figure 4C) and comparably to the ethanol-treated ones ($7.4 \pm 2.2s$, $p > 0.05$ when compared to AG825 and Lapatinib). Likewise, mice pretreated with the broad-selectivity RTK inhibitors were comparable to veh-S, eth-S or eth-TBI mice ($6.1 \pm 2.4s$; $p > 0.05$ when compared to veh-S or eth-S or eth-TBI), whereas mice pretreated with the PDGFR inhibitor performed comparably to the veh-TBI mice ($20.0 \pm 6.5s$; $p > 0.05$ vs veh-TBI; figure 4C). Like in the beam-walk, in the arena-escape tests the improved performance of mice acutely treated with AG825 or Lapatinib was still detectable at 7dpi (figure 4D).

To explore the translational potential of ErbB inhibitors as therapeutic agents for acute TBI, we administered a single dose of 50mg/kg of Lapatinib (an FDA-approved drug, is known to be able to penetrate the brain parenchyma)⁵⁵ or of the alternative ErbB inhibitor AG825, 30min after TBI. Performance of mice in the Beam Walk and Arena Test was evaluated at 2dpi and 7dpi. Interestingly, mice treated with either ErbB inhibitor post-TBI displayed a significantly improved performance in both tests (for the Beam Walk, $10.1 \pm 0.6s$ and $12.5 \pm 2.3s$ at 2dpi; for the Arena escape $6.2 \pm 2.2s$ and $8.4 \pm 1.9s$ for AG825 and Lapatinib, respectively, at 2dpi; $p < 0.05$ compared to sal-TBI). The beneficial effect was persistent at 7dpi.

TBI-induced neuronal loss is prevented by EI and ErbB inhibitors

We then explored the structural counterparts of the reduced behavioral disturbances observed in ethanol-pretreated TBI mice. To this aim, we measured the density of NeuN-positive cells in the injury area ("core", defined by the longitudinal axis of the injury site in coronal sections) and in the penumbra (Supplementary Figure 1; see methods). As control, mice undergoing sham surgery were administered either vehicle (5% PEG400/5%Tween80/90%Saline) alone (veh-S) or ethanol diluted in vehicle (eth-S). In

sham mice, ethanol administration per se did not affect the density of NeuN-positive cells (33.4 ± 3.1 vs $34.9 \pm 2.2/10^4 \mu\text{m}^2$ NeuN⁺ cells in veh-S and eth-S, respectively, $p > 0.05$; figure 4A). On the other hand, 7 days after TBI, cortical samples from veh-TBI mice displayed a primary injury site largely devoid of NeuN⁺ cells ($2.3 \pm 0.9/10^4 \mu\text{m}^2$ NeuN⁺ cells as compared to $33.4 \pm 3.1/10^4 \mu\text{m}^2$ in veh-S mice; $p < 0.001$; figure 4A-B) whereas a significant decrease was observed in the penumbral area ($15.6 \pm 1.1/10^4 \mu\text{m}^2$ vs $35.5 \pm 2.5/10^4 \mu\text{m}^2$ in veh-S and vs $34.4 \pm 2.1/10^4 \mu\text{m}^2$ in eth-S mice; $p < 0.001$; figure 4B-C). Notably, ethanol (diluted in vehicle) pretreated TBI mice displayed a significantly larger population of surviving NeuN⁺ neurons in the injury site ($11.3 \pm 1.3/10^4 \mu\text{m}^2$, $p < 0.01$) and a strong preservation of NeuN⁺ neurons in the penumbra ($27.1 \pm 1.9/10^4 \mu\text{m}^2$, $p < 0.01$ vs both veh-S and veh-TBI; figure 4B-C), further supporting the view of neuroprotective effects of acute ethanol in TBI.

Since our findings had shown that EI results in a significant suppression of TBI-induced ErbB phosphorylation and we have shown that ErbB inhibitors partially recapitulate EI effect, we set out to verify if selective inhibition of ErbB signaling could be sufficient to partially recapitulate EI effect on neuronal survival. To this aim, mice were administered either with two structurally distinct ErbB inhibitors (Lapatinib, 10 mg/kg and AG825, 10mg/kg; since both 50mg/kg and 10mg/kg proved effective in behavioural tests, we selected the lowest dose to ensure specificity) or with a PDGFR inhibitor (CP-673451, 10mg/kg) or with a broad-spectrum RTK inhibitor (including EphR within its selectivity spectrum, LDN-211904, 10mg/kg). All drugs were administered in a single dose before the TBI and mice were then sacrificed after 7 days for the evaluation of the neuronal survival.⁵⁶ Single-dose administration of either drug did not affect apnea time, acute or overall survival (not shown) and all drugs were well tolerated. Although ErbB inhibitors did not affect NeuN⁺ cells in the core (2.3 ± 0.9 and $1.5 \pm 0.3/10^4 \mu\text{m}^2$ for AG825 and Lapatinib, respectively; $p > 0.05$ vs veh-TBI), they significantly preserved neuronal density in the penumbra (21.3 ± 3.2 and $23.3 \pm 4.7/10^4 \mu\text{m}^2$ for AG825 and Lapatinib, as compared to $10.6 \pm 5.1/10^4 \mu\text{m}^2$ in veh-TBI, $p < 0.05$; figure 4A, C), albeit to a lesser extent than what obtained with ethanol. In fact, the broad-spectrum RTK also caused a significant increase in surviving NeuN⁺ cells in the penumbra ($19.9 \pm 3.2/10^4 \mu\text{m}^2$, $p < 0.05$ vs veh-TBI), whereas administration of the PDGFR inhibitor was much less effective ($13.5 \pm 4.5/10^4 \mu\text{m}^2$, $p < 0.05$).

Neither of them, however, helped with preservation of NeuN⁺ cells in the core (2.9 ± 2.4 and $1.9 \pm 0.2/10^4 \mu\text{m}^2$, $p > 0.05$; figure 4A, C).

TBI- induced increase in pErbB2 excitatory synapses on PV interneurons is prevented by EI

ErbB receptors are expressed mainly in inhibitory neurons (in the cortex)³⁵⁻³⁷ including PV interneurons, where they control the strength of excitatory inputs^{38,40} and, in turn, the level of perisomatic inhibition and principal neurons firing.^{39,41} We therefore elected to investigate if ErbB2 phosphorylation in excitatory synapses on PV interneurons was upregulated by TBI and affected by ethanol. PV interneurons were identified by immunostaining for Parvalbumin, and the subpopulation within a 500 μm ROI centered on the injury site and restricted to layer I-IV was considered. On each PV interneuron, the fraction of vGlut2 ErbB2⁺ synapses over the total vGlut2⁺ was counted. The fraction of vGlut2⁺ ErbB2⁺ was comparatively low in sal-S and eth-S ($8 \pm 5\%$ and $5 \pm 4\%$ of all vGlut2⁺ were pErbB2⁺). However, in sal-TBI mice, $57 \pm 21\%$ of vGlu2⁺ on PV interneurons was pErbB2⁺. Notably, in eth-TBI samples, the fraction of vGlut2⁺ ErbB2⁺ synapses on PV interneurons was significantly lower than in sal-TBI samples ($34 \pm 18\%$, $p < 0.05$ vs sal-TBI; figure 6 A, B). Thus, TBI results in ErbB phosphorylation in excitatory synapses on PV interneurons, an effect prevented by concomitant EI. Since EI and TBI reciprocally regulate PV excitatory input, we reasoned that TBI-induced increase in PV activation and perisomatic inhibition may have pathogenic effects, which would be prevented by EI. We therefore set out to manipulate directly PV firing in TBI, to verify if suppression of PV firing may recapitulate EI effect.

Chemogenetic inhibition of PV interneurons partially mimics but does not fully preclude EI-associated neuroprotection

We injected AAV9 encoding either cation or anion-permeable engineered ion channels with orthogonal pharmacology (pharmacologically-selective activation module-PSAM- either excitatory or inhibitory) in the somatosensory cortex of PV-Cre mice.⁴⁸ Mice were then injected 30min before further procedures with either saline alone or the orthogonal agonist (Pharmacologically-selective effector module-PSEM308) and subjected to either sham surgery or TBI. The mice were sacrificed at 7dpi. The density of NeuN⁺ cells at 7dpi

both in the core and in the penumbra of the TBI-induced lesion was used as a read-out. In sham-operated mice, whether administered with saline or PSEM and expressing either excitatory or inhibitory PSAM, NeuN⁺ cell density was comparable at 7dpi (32.4±4.4, 33.4±2.9, 31.9±6.5, 34.2±4.8 NeuN⁺ cells/10⁴μm², p>0.05; figure 6C-E). In saline-pretreated mice (sal-actPSAM-TBI or sal-inhPSAM-TBI, only saline but no PSEM administered), irrespective of the PSAM expression, TBI resulted in almost complete loss of NeuN⁺ cells in the core lesion (2.3±1.4 and 1.9±1.1 NeuN⁺ cells/10⁴μm² in saline-treated mice expressing either actPSAM or inhPSAM, p<0.05 vs sal-S samples; figure 6D, E) and a significant loss of neurons in the penumbral zone (20.1±3.3 and 19.4±4.4 NeuN⁺ cells/10⁴μm²; p<0.05 vs sal-S samples; figure 6D, E). However, when PV interneurons were activated in mice undergoing TBI (PSEM-actPSAM-TBI) the number of NeuN⁺ cells in the core was not affected (3.1±1.4 NeuN⁺ cells/10⁴μm²), but an increased loss of neurons in the penumbra was observed (10.5±2.7 NeuN⁺ cells/10⁴μm²; p<0.05 vs sal-actPSAM-TBI; figure 6D). On the other hand, inhibiting PV interneurons (PSEM-inhPSAM-TBI) produced a significantly higher number of NeuN⁺ cells in the core (8.2±3.1, p<0.05 vs sal-TBI) and a larger preservation of NeuN⁺ cells in the penumbra (24.4±3.2 NeuN⁺ cells/10⁴μm²; p<0.05 vs sal-inhPSAM-TBI). Thus, acute inhibition of PV firing resulted in reduced long-term principal neurons vulnerability whereas activation of PV firing increased neuronal loss.

We then reasoned that if reducing excitation of PV interneurons was the major mechanism of EI-associated neuroprotection and suppressing PV firing would preclude any further beneficial effect of EI. We therefore administered ethanol (5g/kg) together with PSEM in PV-Cre mice expressing the inhibitory PSAM and compared the loss of neurons to that observed in PSEM-only administered mice. Although EI did not improve the neuronal survival in the core lesion when applied together with the chemogenetic inhibition of PV interneurons (9.3±1.4 cells/10⁴μm², p>0.05 vs PSEM alone or EI alone), EI exerted an additional beneficial effect on the preservation of neurons in the penumbra (28.4±1.1 cells/10⁴μm² p<0.05 vs sal-TBI and vs PSEM-TBI; figure 6E), with PSEM+EI being comparable to EI alone (29.5±2.2 cells/10⁴μm², p>0.05 vs PSEM+EI; figure 6E). Likewise, when ethanol was pre-administered to mice in which PV firing was enhanced, it did not enhance survival in the core of the lesion compared to chemogenetics only (4.1±1.7

cells/ $10^4\mu\text{m}^2$, $p>0.05$ vs PSEM) and the PSEM+EI group showed fewer cells than EI alone (7.9 ± 1.2 cells/ $10^4\mu\text{m}^2$). Conversely, the addition of EI to the chemogenetic activation of PV interneurons increased neuronal survival compared to chemogenetic only (17.6 ± 2.4 cells/ $10^4\mu\text{m}^2$ vs 10.5 ± 2.7 NeuN⁺ cells/ $10^4\mu\text{m}^2$ $p<0.05$; figure 6) although did not reach the level of preservation produced by EI alone (27.8 ± 3.4 NeuN⁺ cells/ $10^4\mu\text{m}^2$). Taken together these data indicate that inhibition of PV interneurons does not preclude EI effects, but chemogenetic activation of PV strongly decreases EI-associated neuroprotection.

EI does not reduce overall survival upon TBI

Finally, we retrospectively investigated if EI had a significant effect on the overall survival of experimental mice to TBI. In the sal-TBI and veh-TBI groups, a total of 52 mice underwent TBI procedure and 11 died either during the procedure or met the pre-specified criteria for euthanization (21.2%). In eth-TBI groups, a total of 45 mice underwent TBI, with 12 fatal outcomes (26.7%). When all animals treated with inhibitors were grouped together, 7 fatalities were observed out of 48 which underwent TBI (14.6%). The χ^2 value was 1.067, with $p=0.58$. Therefore, neither ethanol administration nor RTK inhibitors caused a significant increase in overall mortality after TBI.

Discussion

Here we have shown that ethanol pretreatment, resulting in a BAL comparable to the one that was found to be highly correlated with protective effects on TBI patients ($>230\text{mg/dL}$)¹⁰ results in enhanced recovery of sensorimotor skills and in reduced neuronal loss in cortex after blunt TBI, supporting the hypothesis of neuroprotective effects of ethanol observed in clinical series. Lower doses of ethanol were not explored, since we have previously reported that the dose of 1g/kg does not provide protective effects on sensorimotor performance.

We have investigated the involved mechanisms exploiting as entry point the pattern of phosphorylation of multiple RTK after TBI. The activation of RTK may be a physiological, protective response set in motion by the trauma itself (and therefore, in agreement with the classical anti-apoptotic role of RTK, play a protective role in TBI). Under this viewpoint, EI-associated downregulation of the activation of several RTK may reveal that EI may limit

the initial damage and prevent the activation of the protective response in the first place. Since ethanol has powerful GABAergic activities²⁶ and it is an NMDAR antagonist,²⁵ it may prevent excitation-related damage⁷ and limit excitation-related RTK activation (such as the phosphorylation of ErbB;³⁸ or FGFR and EphB phosphorylation).^{31,57} On the other hand, in the CNS RTK may be involved in maladaptive responses to trauma which may be directly pathogenic. In fact, activation of PDGFR has been linked to increased permeability of the Blood-Brain-Barrier after trauma, and the PDGFR inhibitor Imatinib has shown to reduce oedema and reduce cognitive dysfunctions.³³ Furthermore, activation of the RTK EphA2 has been linked to increased BBB dysfunction and neuronal loss in a stroke model.⁵⁸ Thus, although the RTK activation pattern reveals the breath of EI impact on TBI-associated signaling events, the specific role of each RTK (and associated cascades) in EI-associated neuroprotection should be investigated in a case-by-case manner. Of note, some cascades endowed with pathogenic potential are not modulated by EI: Tie-2 phosphorylation, which is linked to reduced permeability of endothelial barriers, is not significantly modified by ethanol pretreatment.³⁴ Likewise, HGFR signaling is strongly activated by TBI but not affected by EI. The role of HGFR in TBI has never been explored before, but its involvement in enhancing NMDAR⁵⁹ may suggest a potential involvement.

Notably, several of the TBI-activated RTK are also involved (although not exclusively) in the regulation of synaptic events: EphB signaling can potentiate NMDAR currents⁶⁰ and may therefore enhance glutamate toxicity in the acute phase of TBI. The activation of other RTK, such as FGFR1 and ErbB family, is known to control protein clustering at inhibitory synapses^{61,62} and excitatory inputs on interneurons,²⁸ respectively. Thus, our RTK screening reveals that EI may affect strongly events unfolding at synaptic level after trauma and may identify new targets for intervention at this level.

Focusing on the ErbB receptor family, we have shown that TBI induces the phosphorylation of ErbB receptors in excitatory synapses and that specific inhibitors of ErbB are able to recapitulate a significant fraction of EI-associated neuroprotection. ErbB family expression pattern has been originally reported to include pyramidal cells as well as inhibitory interneurons. However, recent data obtained by *in situ* hybridization and reporter expression based on ErbB4 endogenous promoter³⁵⁻³⁸ as well as cell-specific knockout

experiments⁴⁰ have demonstrated that ErbB4 expression is restricted in the cortex only to inhibitory interneurons (although ErbB4 is expressed in several non-GABAergic subpopulations in subcortical structures) and that ErbB4 is dispensable for the function of excitatory synapses between pyramidal neurons.³⁶ Although data on the expression of ERbB2 and ErbB3 are not as detailed, ERbB family members signal either as ERbB4 homodimers or as heterodimers of ErbB4, ErbB3 and Erbb2,⁶³ and therefore their expression is predicted to be comparable. Thus, we show that TBI induces the phosphorylation of ErbB in excitatory synapses on inhibitory interneurons. Among inhibitory interneurons, ErbB expression in PV interneurons has been shown to be highly relevant for the control of the function of these cells in normal cortex^{39, 40} and under pathological conditions.^{64, 65}

The effect of EI on ErbB and PV activation may appear paradoxical, considering the GABAergic action of ethanol. However, ErbB phosphorylation on interneurons has been shown to be homeostatically regulated: reduced cortical excitation leads to the decrease in ErbB phosphorylation in PV interneurons, de-potentialization and de-stabilization of excitatory synapses and ultimately reduce PV activation.^{27, 66} Reciprocally, activation of ErbB results in the insertion of AMPAR and increase excitation to inhibitory interneurons,²⁷ although, the ratio between AMPAR and NMDAR may change significantly.³⁸ Thus, following TBI-associated depolarization, upregulation of ErbB in excitatory synapses on PV interneurons may result in the upregulation of perisomatic inhibition, whereas concomitant EI may prevent it and leave PV interneurons at their basal state of excitatory input. We speculate that upregulation of ErbB phosphorylation may be a homeostatic event triggered by TBI-triggered excitation and may lead to increased PV excitation after TBI. In fact, ErbB receptors are activated by the extracellular domain of several isoforms of neuregulins (Nrg). Immature Nrg are transmembrane proteins (widely expressed in principal neurons)⁶⁷ whose extracellular N-terminal domain is released upon activity-dependent proteolysis⁶⁸ and activates ErbB family receptor signaling.²⁸ Nrg1 has been shown to act directly on ErbB receptors localized on interneurons to enhance the release of GABA.^{67, 69} In fact, seizure activity strongly enhances the activation of the Neuregulin1/ErbB signaling unit,⁷⁰ whereas deletion of ErbB4 in PV interneurons increases

seizures susceptibility.⁶⁷ On the other hand, administration of soluble Nrg1 rapidly upregulates excitatory inputs in PV interneurons via ErbB4 signaling.²⁷

If excitatory input to PV is upregulated as consequence of TBI, and prevented by EI, downregulation of PV firing would mimic, at least partially, EI effects. Our chemogenetic manipulation of PV firing, in fact, demonstrates that while increasing PV firing is detrimental, decreasing it results in an improved neuronal survival. This result may apparently contradict the current model of hyperexcitability and excitotoxicity-induced neuronal death in TBI.⁷¹ Although a number of neurons may be directly killed by excitotoxic mechanism at the instance of trauma, it must be noted that, although cortical neurons subject to TBI, develop a hyperexcitable phenotype several weeks after trauma.^{71,72} On the other hand, recordings of sensory-evoked responses in multiple TBI models have revealed that cortical neurons are largely hypo-active,⁶⁸ and do not respond to sensory stimulation in agreement with increased inhibition.⁷³⁻⁷⁵ This effect has been hypothesized to contribute to the generation of TBI-associated acute neurological deficits.⁷⁵ Thus, cortical neurons may be actually hypoactive soon after trauma, an effect that may be related to increased inhibition (in fact, activation of PV interneurons have been shown to be sufficient to completely shutting down the firing of principal cells).⁴¹

Although the mechanisms linking neuronal hypoactivity to cell death in TBI require further elucidation, the current evidence is in agreement with the view that preventing neuronal silencing by either preventing ErbB upregulation (as in the case of EI) or reducing perisomatic inhibition (as in the case of chemogenetic inhibition of PV interneurons) may contribute to neuroprotection (figure 7). In fact, neuronal activity has been shown to increase resilience of neurons to several toxic agents and to neurodegenerative processes through activity-controlled neuroprotective transcriptional programs^{46, 76-79} and silencing neurons render them more sensitive to the degenerative processes (figure 6).⁴⁶

Nevertheless, the neuroprotective mechanisms of EI may extend beyond the limitation of post-TBI inhibition. In fact, chemogenetic suppression of PV interneurons does not preclude EI effects and EI enhances neuronal survival even in case of strong activation of PV interneurons. Since ethanol is both a GABA agonist^{26, 51} as well as an NMDAR

antagonist,²⁵ EI-associated neuroprotection may include direct decrease of excitability at the instance of trauma, reduced excitotoxicity through glutamate receptor inhibition as well as modulatory effects on the neuroimmunological response.²⁰

Intriguingly, blockade of ErbB2 signaling by trastuzumab enhances peripheral nerve regeneration after acute or chronic damage.⁸⁰ However, the mechanism involved requires the interaction between Neuroligin expressed on axons and ErbB2 and EGFR expressed on Schwann cells, whose interactions control Schwann cell dedifferentiation after injury and may therefore be independent of potential effects in the CNS.⁸¹ Nevertheless, in polytrauma patients suffering from central and peripheral nervous system injuries, targeting of ErbB signaling would be highly attractive for the delivery of a double benefit.

The present work has been performed, in agreement with ethical guidelines for animal experimentation, providing the animals with the best supportive care and with the opportune measures to prevent unnecessary pain. This has required the administration of O₂ during the procedure and the treatment of animals with buprenorphine. Although these conditions are not comparable to those experienced by human patients after TBI, we have provided evidence showing that the combination of ethanol and buprenorphine did not result in additional respiratory suppression and PaCO₂ levels were comparable in ethanol and saline-pretreated animals. In addition, administration of O₂ has been shown to have neuroprotective effects in a TBI+hemorrhagic shock model.⁸² Although administration of O₂ may have affected the disease process examined in our model, it must be stressed that neuroprotection was observed with hypoxemia lasting for no less than 2h, whereas our animals were returned to ambient air within 15min of the trauma. Furthermore, any protective effect of O₂ would have been balanced across groups, since PaO₂ was comparable across treatment groups.

We have identified a previously unrecognized strong effect of TBI on ethanol metabolism leading to distinct pharmacokinetics in eth-TBI vs eth-S, which resulted in significantly higher levels of ethanol assessed 3h (but not 15min after TBI). Since the kinetics of the BAL are different in terms of metabolism, they could not be matched by increasing the dose administered to the eth-S group. In addition, administration of doses larger than 5g/kg

(32% ethanol v/v) may be against ethically acceptable practices for animal experimentations since they may cause mucosal damage or unacceptably high mortality rates. TBI has been previously shown to affect liver biochemistry and gene expression,^{83, 84} which may affect drug metabolism;⁸⁵ in addition, TBI decreases perfusion of the liver (and of other abdominal organs).⁸⁶ These factors may contribute to the altered pharmacokinetics of ethanol in TBI and may contribute to accounting for the increased BAL values. Thus, the difference in BAL obtained by administering the same ethanol dose in eth-S and eth-TBI mice should be considered a limitation of the present study (and further investigations of TBI-induced changes in pharmacokinetics are warranted). However, it is noteworthy that for no RTK the effect of eth-S and eth-TBI was qualitatively divergent (i.e., eth-S and eth-TBI either showed both to decrease RTK [such as for ErbB2, ErbB3, FGFR1, Flt3, PDGFR] activation or to have no or limited effect on RTK activation [like for HGFR, FGFR3, EphA2]) and there is no evidence suggesting that higher levels of ethanol found in eth-TBI mice may have a radically different or opposite effect on RTK than those observed in eth-S mice. Therefore, the difference in BAL between eth-S and eth-TBI does not negate the main conclusions of the paper. Since patients with very high BAL have been reported⁸⁷ and in clinical series, ethanol has been reported to be protective for the groups with the highest BAL¹⁰ the effect of high-dose ethanol on TBI remains relevant for clinical and translational investigations.

The translational potential of our finding is supported by the identification of Lapatinib (a FDA-approved drug for the treatment of breast cancer) as a potential neuroprotective agent when administered before but, most importantly, also after the trauma. Lapatinib pharmacokinetics have been described and partial, dose-dependent penetration of the brain has been shown in murine models.^{54, 88} Penetration of brain parenchyma has been shown to be enhanced when Blood-Brain-Barrier (BBB) is disrupted,⁸⁹ suggesting that it may reach therapeutically relevant concentrations in murine and human brains after TBI. We have supported the Lapatinib data with a second ErbB inhibitor, AG825. Although AG825 has been previously used in vivo,^{90, 91} currently no pharmacokinetic data about AG825 penetration of the BBB are available.

In conclusion, our data provide support to the clinical evidence of a neuroprotective effect of high-dose ethanol in TBI, showing a mechanistic effect targeting multiple signaling cascades including, importantly, RTK signaling, controlling the activity and plasticity of inhibitory interneurons. Direct modulation of the pathways that control inhibitory microcircuits may therefore offer a new approach for understanding and targeting TBI pathogenic pathways.

Acknowledgement

This work has been supported by the Deutsche Forschungsgemeinschaft as part of the Collaborative Research Center 1149 “Danger Response, Disturbance Factors and Regenerative Potential after Acute Trauma”. FR and RR are also supported by the ERANET-NEURON initiative “External Insults to the Nervous System” as part of the MICRONET consortium and by the Baustein program of the Medical Faculty of Ulm University.

Conflict of Interest

The authors declare no conflict of interest.

References

1. Coronado, V.G., Xu, L., Basavaraju, S.V., McGuire, L.C., Wald, M.M., Faul, M.D., Guzman, B.R., and Hemphill, J.D.; Centers for Disease Control and Prevention (CDC). (2011). Surveillance for traumatic brain injury-related deaths--United States, 1997-2007. *MMWR Surveill Summ.* 60, 1-32.
2. Bruns, J., and Hauser, W.A. (2003). The epidemiology of traumatic brain injury: a review. *Epilepsia* 44(S10), 2-10.
3. Leo P, and McCrea M.(2016). Epidemiology. In: *Translational Research in Traumatic Brain Injury*. Laskowitz D and Grant G (eds). CRC Press/Taylor and Francis Group : Boca Raton (FL), chapter 1.
4. Zaloshnja, E., Miller T., Langlois J. A., and Selassie, A. W. (2005). Prevalence of long-term disability from traumatic brain injury in the civilian population of the United States. *The Journal of head trauma rehabilitation.* 23, 394-400.
5. Stein, C.S., Georgoff, P., Meghan, S., Mizra, K., and Sonnad, S.S. (2010). 150 years of treating severe traumatic brain injury: a systematic review of progress in mortality. *J Neurotrauma.* 27, 1343-1353.
6. Savola, O., Niemelä, O., and Hillbom, M. (2005). Alcohol intake and the pattern of trauma in young adults and working aged people admitted after trauma. *Alcohol Alcohol.* 40, 269-273.
7. Brennan, J.H., Bernard, S., Cameron, P.A., Rosenfeld, J.V., and Mitra, B. (2015). Ethanol and isolated traumatic brain injury. *J Clin Neurosci.* 22, 1375-1381.
8. Raj, R., Skrifvars, M.B., Kivisaari, R., Hernesniemi, J., Lappalainen, J., and Siironen, J. (2015). Acute alcohol intoxication and long-term outcome in patients with traumatic brain injury. *J. Neurotrauma.* 32, 95-100.
9. Raj, R., Mikkonen, E.D., Siironen, J., Hernesniemi, J., Lappalainen, J., and Skrifvars, M.B. (2016). Alcohol and mortality after moderate to severe traumatic brain injury: a meta-analysis of observational studies. *J Neurosurg.* 124, 1684-1692.
10. Berry, C., Ley, E.J., Margulies, D.R., Mirocha, J., Bukur, M., Malinoski, D., and Salim, A. (2011). Correlating the blood alcohol concentration with outcome after traumatic brain injury: too much is not a bad thing. *Am. Surg.* 77, 1416-1419.

11. Salim, A., Teixeira, P., Ley, E.J., DuBose, J., Inaba, K., and Margulies, D.R. (2009). Serum ethanol levels: predictor of survival after severe traumatic brain injury. *J Trauma*. 67, 697-703.
12. Wang, T., Chou, D.Y., Ding, J.Y., Fredrickson, V., Peng, C., Schafer, S., Guthikonda, M., Kreipke, C., Rafols, J.A., and Ding, Y. (2013). Reduction of brain edema and expression of aquaporins with acute ethanol treatment after traumatic brain injury. *J Neurosurg*. 118, 390-396.
13. Joseph, B., Khalil, M., Pandit, V., Kulvatunyou, N., Zangbar, B., O'Keeffe, T., Asif, A., Tang, A., Green, D.J., Gries, L., Friese, R.S., and Rhee, P. (2015). Adverse effects of admission blood alcohol on long-term cognitive function in patients with traumatic brain injury. *J Trauma Acute Care Surg*. 78, 403-408.
14. Pandit, V., Patel, N., Rhee, P., Kulvatunyou, N., Aziz, H., Green, D.J., O'Keeffe, T., Zangbar, B., Tang, A., Gries, L., Friese, R.S., and Joseph, B. (2014). Effect of alcohol in traumatic brain injury: is it really protective? *J Surg Res*. 190, 634-639.
15. Lange, R.T., Iverson, G.L., and Franzen, M.D. (2008). Effects of day-of-injury alcohol intoxication on neuropsychological outcome in the acute recovery period following traumatic brain injury. *Arch Clin Neuropsychol*. 23, 809-822.
16. Schutte, C., and Hanks, R. (2010). Impact of the presence of alcohol at the time of injury on acute and one-year cognitive and functional recovery after traumatic brain injury. *Int J Neurosci*. 120, 551-556.
17. Kaplan, C.P. and Corrigan, J.D. (1992). Effect of blood alcohol level on recovery from severe closed head injury. *Brain Inj*. 6, 337-349.
18. Wu, W., Tian, R., Hao, S., Xu, F., Mao, X., and Liu, B. (2014). A pre-injury high ethanol intake in rats promotes brain edema following traumatic brain injury. *Br J Neurosurg*. 28, 739-745.
19. Vaagenes, I.C., Tsai, S.Y., Ton, S.T., Husak, V.A., McGuire, S.O., O'Brien, T.E., and Kartje, G.L. (2015). Binge ethanol prior to traumatic brain injury worsens sensorimotor functional recovery in rats. *PLoS One*, 10, e0120356.

20. Chandrasekar, A., Heuvel, F.O., Palmer, A., Linkus, B., Ludolph, A.C., Boeckers, T.M., Relja, B., Huber-Lang, M., and Roselli, F. (2017). Acute ethanol administration results in a protective cytokine and neuroinflammatory profile in traumatic brain injury. *Int Immunopharmacol.* 51, 66-75.
21. Kelly, D.F., Lee, S.M., Pinanong, P.A., and Hovda, D.A. (1997). Paradoxical effects of acute ethanolism in experimental brain injury. *J Neurosurg.* 86, 876-882.
22. Janis, L.S., Hoane, M.R., Conde, D., Fulop, Z., and Stein, D.G. (1998). Acute ethanol administration reduces the cognitive deficits associated with traumatic brain injury in rats. *J Neurotrauma.* 15, 105-115.
23. Goodman, M.D., Makley, A.T., Campion, E.M., Friend, L.A., Lentsch, A.B., and Pritts, T.A. (2013). Preinjury alcohol exposure attenuates the neuroinflammatory response to traumatic brain injury. *J Surg Res.* 184, 1053-1058.
24. Katada, R., Nishitani, Y., Honmou, O., Mizuo, K., Okazaki, S., Tateda, K., Watanabe, S., and Matsumoto, H. (2012). Expression of aquaporin-4 augments cytotoxic brain edema after traumatic brain injury during acute ethanol exposure. *Am J Pathol.* 180, 17-23.
25. Criswell, H.E., Ming, Z., Pleasant, N., Griffith, B.L., Mueller, R.A., and Breese, G.R. (2004). Macrokinetic analysis of blockade of NMDA-gated currents by substituted alcohols, alkanes and ethers. *Brain Res.* 1015, 107-113.
26. Kumar, S., Porcu, P., Werner, D.F., Matthews, D.B., Diaz-Granados, J.L., Helfand, R.S., and Morrow, A.L. (2009). The role of GABA(A) receptors in the acute and chronic effects of ethanol: a decade of progress. *Psychopharmacology (Berl).* 205, 529-564.
27. Sun, Y., Ikrar, T., Davis, M.F., Gong, N., Zheng, X., Luo, Z.D., Lai, C., Mei, L., Holmes, T.C., Gandhi, S.P., and Xu, X. (2016). Neuregulin-1/ErbB4 Signaling Regulates Visual Cortical Plasticity. *Neuron.* 92, 160-173.
28. Mei, L., and Nave, K.A. (2014). Neuregulin-ERBB signaling in the nervous system and neuropsychiatric diseases. *Neuron.* 83, 27-49.
29. Gupta, V.K., You, Y., Gupta, V.B., Klistorner, A., and Graham, S.L. (2013). TrkB receptor signalling: implications in neurodegenerative, psychiatric and proliferative disorders. *Int J Mol Sci.* 14, 10122-42.

30. Fourgeaud, L., Través, P.G., Tufail, Y., Leal-Bailey, H., Lew, E.D., Burrola, P.G., Callaway, P., Zagórska, A., Rothlin, C.V., Nimmerjahn, A., and Lemke, G. (2016). TAM receptors regulate multiple features of microglial physiology. *Nature*. 532, 240-244.
31. Sheffler-Collins, S.I., and Dalva, M.B. (2012). EphBs: an integral link between synaptic function and synaptopathies. *Trends Neurosci*. 35, 293-304.
32. Guillemot, F., and Zimmer, C. (2011). From cradle to grave: the multiple roles of fibroblast growth factors in neural development. *Neuron*. 71, 574-588.
33. Su, E.J., Fredriksson, L., Kanzawa, M., Moore, S., Folestad, E., Stevenson, T.K., Nilsson, I., Sashindranath, M., Schielke, G.P., Warnock, M., Ragsdale, M., Mann, K., Lawrence, A.L., Medcalf, R.L., Eriksson, U., Murphy, G.G. and Lawrence, D.A. (2015). Imatinib treatment reduces brain injury in a murine model of traumatic brain injury. *Front Cell Neurosci* 9, 385.
34. Gurnik, S., Devraj, K., Macas, J., Yamaji, M., Starke, J., Scholz, A., Sommer, K., Di Tacchio, M., Vutukuri, R., Beck, H., Mittelbronn, M., Foerch, C., Pfeilschifter, W., Liebner, S., Peters, K.G., Plate, K.H., and Reiss, Y. (2016). Angiopoietin-2-induced blood-brain barrier compromise and increased stroke size are rescued by VE-PTP-dependent restoration of Tie2 signaling. *Acta Neuropathol*. 31, 753-773.
35. Bean, J.C., Lin, T.W., Sathyamurthy, A., Liu, F., Yin, D.M., Xiong, W.C., and Mei, L. (2014). Genetic labeling reveals novel cellular targets of schizophrenia susceptibility gene: distribution of GABA and non-GABA ErbB4-positive cells in adult mouse brain. *J Neurosci*. 34, 13549-66.
36. Fazzari, P., Paternain, A.V., Valiente, M., Pla, R., Luján, R., Lloyd, K., Lerma, J., Marín, O., and Rico, B. (2010). Control of cortical GABA circuitry development by Nrg1 and ErbB4 signalling. *Nature*. 464, 1376-1380.
37. Neddens, J., Fish, K.N., Tricoire, L., Vullhorst, D., Shamir, A., Chung, W., Lewis, D.A., McBain, C.J., and Buonanno, A. (2011). Conserved interneuron-specific ErbB4 expression in frontal cortex of rodents, monkeys, and humans: implications for schizophrenia. *Biol Psychiatry*. 70, 636-45.

38. Vullhorst, D., Mitchell, R.M., Keating, C., Roychowdhury, S., Karavanova, I., Tao-Cheng, J.H., and Buonanno, A. (2015). A negative feedback loop controls NMDA receptor function in cortical interneurons via neuregulin 2/ErbB4 signalling. *Nat Commun.* 6.
39. Wen, L., Lu, Y.S., Zhu, X.H., Li, X.M., Woo, R.S., Chen, Y.J., Yin, D.M., Lai, C., Terry, A.V., Vazdarjanova, A., and Xiong, W.C. (2010). Neuregulin 1 regulates pyramidal neuron activity via ErbB4 in parvalbumin-positive interneurons. *Proceedings of the National Academy of Sciences.* 107,1211-1216.
40. Yin, D.M., Sun, X.D., Bean, J.C., Lin, T.W., Sathyamurthy, A., Xiong, W.C., Gao, T.M., Chen, Y.J., and Mei, L. (2013). Regulation of spine formation by ErbB4 in PV-positive interneurons. *J Neurosci.* 33, 19295-303.
41. Atallah, B.V., Bruns, W., Carandini, M., and Scanziani, M. (2012). Parvalbumin-expressing interneurons linearly transform cortical responses to visual stimuli. *Neuron.* 73, 159-70.
42. Jacobi, N., Seeboeck, R., Hofmann, E., and Eger, A. (2017). ErbB Family Signalling: A Paradigm for Oncogene Addiction and Personalized Oncology. *Cancers (Basel)* 9, pii: E33.
43. Flierl, M.A., Stahel, P.F., Beauchamp, K.M., Morgan, S.J., Smith, W.R., and Shohami, E. (2009). Mouse closed head injury model induced by a weight-drop device. *Nat Protoc.* 4, 1328-1337.
44. Luong, T.N., Carlisle, H.J., Southwell, A., and Patterson, P.H. (2011). Assessment of motor balance and coordination in mice using the balance beam. *J Vis Exp.* 10, pii: 2376.
45. Zimprich, A., Garrett, L., Deussing, J.M., Wotjak, C.T., Fuchs, H., Gailus-Durner, V., de Angelis, M.H., Wurst, W., and Hölter, S.M. (2014). A robust and reliable non-invasive test for stress responsivity in mice. *Front Behav Neurosci.* 8.
46. Saxena, S., Roselli, F., Singh, K., Leptien, K., Julien, J.P., Gros-Louis, F., and Caroni, P. (2013). Neuroprotection through excitability and mTOR required in ALS motoneurons to delay disease and extend survival. *Neuron.* 80, 80-96.

47. Karunakaran, S., Chowdhury, A., Donato, F., Quairiaux, C., Michel, C.M., and Caroni, P. (2016). PV plasticity sustained through D1/5 dopamine signaling required for long-term memory consolidation. *Nat Neurosci.* 19, 454-464.
48. Magnus, C.J., Lee, P.H., Atasoy, D., Su, H.H., Looger, L.L., and Sternson, S.M. (2011). Chemical and genetic engineering of selective ion channel-ligand interactions. *Science.* 333, 1292-1296.
49. Schwarzkopf, T.M., Horn, T., Lang, D., and Klein, J. (2013). Blood gases and energy metabolites in mouse blood before and after cerebral ischemia: the effects of anesthetics. *Exp Biol Med (Maywood).* 238, 84-9.
50. Papa, L., Brophy, G.M., Welch, R.D., Lewis, L.M., Braga, C.F., Tan, C.N., Ameli, N.J., Lopez, M.A., Haeussler, C.A., Mendez-Giordano, D.I, Silvestri, S., Giordano, P., Weber, K.D., Hill-Pryor, C., and Hack, D.C. (2016). Time course and diagnostic accuracy of glial and neuronal blood biomarkers GFAP and UCH-L1 in a large cohort of trauma patients with and without mild traumatic brain injury. *JAMA Neurol.* 73, 551-560.
51. Huang, X.J., Glushakova, O., Mondello, S., Van, K., Hayes, R.L., and Lyeth, B.G. (2015). Acute Temporal Profiles of Serum Levels of UCH-L1 and GFAP and Relationships to Neuronal and Astroglial Pathology following Traumatic Brain Injury in Rats. *J Neurotrauma.* 32, 1179-1189.
52. Gerecke, K.M., Wyss, J.M., Karavanova, I., Buonanno, A., and Carroll, S.L. (2001). ErbB transmembrane tyrosine kinase receptors are differentially expressed throughout the adult rat central nervous system. *J Comp Neurol.* 433, 86-100.
53. Thompson, M., Lauderdale, S., Webster, M.J., Chong, V.Z., McClintock, B., Saunders, R., and Weickert, C.S. (2007). Widespread expression of ErbB2, ErbB3 and ErbB4 in non-human primate brain. *Brain Res.* 30, 95-109.
54. Polli, J.W., Humphreys, J.E., Harmon, K.A., Castellino, S., O'Mara, M.J., Olson, K.L., John-Williams, L.S., Koch, K.M., and Serabjit-Singh, C.J. (2008). The role of efflux and uptake transporters in [N-{3-chloro-4-[(3-fluorobenzyl)oxy]phenyl}-6-[5-([2-(methylsulfonyl)ethyl]amino)methyl)-2-furyl]-4-quinazolinamine (GW572016, lapatinib) disposition and drug interactions. *Drug Metab Dispos.* 36, 695-701.

55. Hudachek, S.F., and Gustafson, D.L. (2013). Physiologically based pharmacokinetic model of lapatinib developed in mice and scaled to humans. *J Pharmacokinet Pharmacodyn.* 40, 157-76.
56. Qiao, L., Choi, S., Case, A., Gainer, T.G., Seyb, K., Glicksman, M.A., Lo, D.C., Stein, R.L., and Cuny, G.D. (2009). Structure-activity relationship study of EphB3 receptor tyrosine kinase inhibitors. *Bioorg Med Chem Lett.* 19, 6122-6126.
57. Flajolet, M., Wang, Z., Futter, M., Shen, W., Nuangchamnong, N., Bendor, J., Wallach, I., Nairn, A.C., Surmeier, D.J., and Greengard, P. (2008). FGF acts as a co-transmitter through adenosine A(2A) receptor to regulate synaptic plasticity. *Nat Neurosci.* 11, 1402-1409.
58. Thundyil, J., Manzanero, S., Pavlovski, D., Cully, T.R., Lok, K.Z., Widiapradja, A., Chunduri, P., Jo, D.G., Naruse, C., Asano, M., Launikonis, B.S., Sobey, C.G., Coulthard, M.G., and Arumugam, T.V. (2013). Evidence that the EphA2 receptor exacerbates ischemic brain injury. *PLoS One.* 8, e53528.
59. Akimoto, M., Baba, A., Ikeda-Matsuo, Y., Yamada, M.K., Itamura, R., Nishiyama, N., Ikegaya, Y., Matsuki, N. (2004). Hepatocyte growth factor as an enhancer of NMDA currents and synaptic plasticity in the hippocampus. *Neuroscience.* 128, 155-62.
60. Nolt, M.J., Lin, Y., Hruska, M., Murphy, J., Sheffler-Colins, S.I., Kayser, M.S., Passer, J., Bennett, M.V., Zukin, R.S., and Dalva, M.B. (2011). EphB controls NMDA receptor function and synaptic targeting in a subunit-specific manner. *Neurosci.* 31, 5353-5364.
61. Kriebel, M., Metzger, J., Trinks, S., Chugh, D., Harvey, R.J., Harvey, K., and Volkmer, H. (2011). The cell adhesion molecule neurofascin stabilizes axo-axonic GABAergic terminals at the axon initial segment. *J Biol Chem.* 286, 24385-24393.
62. Wuchter, J., Beuter, S., Treindl, F., Herrmann, T., Zeck, G., Templin, M.F., and Volkmer, H. (2012). A comprehensive small interfering RNA screen identifies signaling pathways required for gephyrin clustering. *J Neurosci.* 32, 14821-14834.
63. Mei, L., and Xiong, W.C. (2008). Neuregulin 1 in neural development, synaptic plasticity and schizophrenia. *Nature Reviews Neuroscience.* 9,437-452.

64. Guan, Y.F., Wu, C.Y., Fang, Y.Y., Zeng, Y.N., Luo, Z.Y., Li, S.J., Li, X.W., Zhu, X.H., Mei, L., and Gao, T.M. (2015). Neuregulin 1 protects against ischemic brain injury via ErbB4 receptors by increasing GABAergic transmission. *Neuroscience*. 307, 151-9.
65. Zhang, H., Zhang, L., Zhou, D., He, X., Wang, D., Pan, H., Zhang, X., Mei, Y., Qian, Q., Zheng, T., Jones, F.E., and Sun, B. (2017). Ablating ErbB4 in PV neurons attenuates synaptic and cognitive deficits in an animal model of Alzheimer's disease. *Neurobiol Dis*. 106, 171-180.
66. Lu, Y., Sun, X.D., Hou, F.Q., Bi, L.L., Yin, D.M., Liu, F., Chen, Y.J., Bean, J.C., Jiao, H.F., Liu, X., Li, B.M., Xiong, W.C., Gao, T.M., and Mei, L. (2014). Maintenance of GABAergic activity by neuregulin 1-ErbB4 in amygdala for fear memory. *Neuron*. 84, 835-846.
67. Tamura, H., Kawata, M., Hamaguchi, S., Ishikawa, Y., and Shiosaka, S. (2012) Processing of neuregulin-1 by neuropsin regulates GABAergic neuron to control neural plasticity of the mouse hippocampus. *J Neurosci*. 32, 12657-72.
68. Iwakura, Y., Wang, R., Inamura, N., Araki, K., Higashiyama, S., Takei, N., and Nawa H. (2017). Glutamate-dependent ectodomain shedding of neuregulin-1 type II precursors in rat forebrain neurons. *PLoS One*. 12, e0174780.
69. Woo, R.S., Li, X.M., Tao, Y., Carpenter-Hyland, E., Huang, Y.Z., Weber, J., Neiswender, H., Dong, X.P., Wu, J., Gassmann, M., Lai, C., Xiong, W.C., Gao, T.M., and Mei, L. (2007). Neuregulin-1 enhances depolarization-induced GABA release. *Neuron*. 54, 599-610.
70. Tan, G.H., Liu, Y.Y., Hu, X.L., Yin, D.M., Mei, L., and Xiong, Z.Q. (2011). Neuregulin 1 represses limbic epileptogenesis through ErbB4 in parvalbumin-expressing interneurons. *Nat Neurosci*. 15, 258-66.1
71. Carron, S.F., Alwis, D.S., and Rajan, R. (2016). Traumatic Brain Injury and Neuronal Functionality Changes in Sensory Cortex. *Front Syst Neurosci*. 10, 47.
72. Alwis, D.S., Yan, E.B., Morganti-Kossmann, M.C., and Rajan, R. (2012). Sensory cortex underpinnings of traumatic brain injury deficits. *PLoS One*, 7.
73. Johnstone, V.P., Yan, E.B., Alwi, D.S., and Rajan, R. (2013). Cortical hypoexcitation defines neuronal responses in the immediate aftermath of traumatic brain injury. *PLoS One* 8, e63454.

74. Allitt, B.J., Iva, P., Yan, E.B., and Rajan, R. (2016). Hypo-excitation across all cortical laminae defines intermediate stages of cortical neuronal dysfunction in diffuse traumatic brain injury. *Neurosci.* 334, 290-308.
75. Johnstone, V.P., Shultz, S.R., Yan, E.B., O'Brien, T.J., and Rajan, R. (2014). The acute phase of mild traumatic brain injury is characterized by a distance-dependent neuronal hypoactivity. *J Neurotrauma.* 31, 1881-1895.
76. Bading, H. (2013). Nuclear calcium signalling in the regulation of brain function. *Nat Rev Neurosci.* 14, 593-608.
77. Roselli, F., and Caroni, P. (2015). From intrinsic firing properties to selective neuronal vulnerability in neurodegenerative diseases. *Neuron* 85, 901-910.
78. Zhang, S.J., Buchthal, B., Lau, D., Hayer, S., Dick, O., Schwaninger, M., Veltkamp, R., Zou, M., Weiss, U., and Bading, H. (2011). A signaling cascade of nuclear calcium-CREB-ATF3 activated by synaptic NMDA receptors defines a gene repression module that protects against extrasynaptic NMDA receptor-induced neuronal cell death and ischemic brain damage. *J Neurosci.* 31, 4978-90.
79. Zhang, S.J., Zou, M., Lu, L., Lau, D., Ditzel, D.A., Delucinge-Vivier, C., Aso, Y., Descombes, P., and Bading, H. (2009). Nuclear calcium signaling controls expression of a large gene pool: identification of a gene program for acquired neuroprotection induced by synaptic activity. *PLoS Genet.* 5.
80. Hendry, J.M., Alvarez-Veronesi, M.C., Placheta, E., Zhang, J.J., Gordon, T., and Borschel, G.H. (2016). ErbB2 blockade with Herceptin (trastuzumab) enhances peripheral nerve regeneration after repair of acute or chronic peripheral nerve injury. *Ann Neurol.* 80, 112-126.
81. Hendry, J.M., Alvarez-Veronesi, M.C., Placheta, E., Zhang, J.J., Gordon, T. and Borschel, G.H. (2016). ErbB2 blockade with Herceptin (trastuzumab) enhances peripheral nerve regeneration after repair of acute or chronic peripheral nerve injury. *Ann Neurol.* 80, 112-126.
82. Boerboom, A., Dion, V., Chariot, A., and Franzen, R. (2017). Molecular Mechanisms Involved in Schwann Cell Plasticity. *Front Mol Neurosci.* 10, 38.

83. Blasiole, B., Bayr, H., Vagni, V.A., Janesko-Feldman, K., Cheikhi, A., Wisniewski, S.R., Long, J.B., Atkins, J., Kagan, V., and Kochanek, P.M. (2013). Effect of hyperoxia on resuscitation of experimental combined traumatic brain injury and hemorrhagic shock in mice. *Anesthesiology*. 118, 649-63.
84. Kalsotra, A., Turman, C.M., Dash, P.K., and Strobel, H.W. (2003). Differential effects of traumatic brain injury on the cytochrome p450 system: a perspective into hepatic and renal drug metabolism. *J Neurotrauma*. 20, 1339-50.
85. Nizamutdinov, D., DeMorrow, S., McMillin, M., Kain, J., Mukherjee, S., Zeitouni, S., Frampton, G., Bricker, P.C., Hurst, J., and Shapiro, L.A. (2017). Hepatic alterations are accompanied by changes to bile acid transporter-expressing neurons in the hypothalamus after traumatic brain injury. *Sci Rep*. 7.
86. Boucher, B.A., and Hanes, S.D. (1998). Pharmacokinetic alterations after severe head injury. Clinical relevance. *Clin Pharmacokinet*. 35, 209-21.
87. Yuan, X.Q., Wade, C.E., Prough, D.S., and DeWitt, D.S. (1990). Traumatic brain injury creates biphasic systemic hemodynamic and organ blood flow responses in rats. *J Neurotrauma*. 7, 141-53.
88. Afshar, M., Netzer, G., Salisbury-Afshar, E., Murthi, S., and Smith, G.S. (2016). Injured patients with very high blood alcohol concentrations. *Injury*. 47,83-88.
89. Polli, J.W., Humphreys, J.E., Harmon, K.A., Castellino, S., O'mara, M.J., Olson, K.L., John-Williams, L.S., Koch, K.M., and Serabjit-Singh, C.J. (2008). The role of efflux and uptake transporters in N-{3-chloro-4-[(3-fluorobenzyl) oxy] phenyl}-6-[5-({[2-(methylsulfonyl) ethyl] amino} methyl)-2-furyl]-4-quinazolinamine (GW572016, lapatinib) disposition and drug interactions. *Drug Metabolism and Disposition*. 36, 695-701.
90. Morikawa, A., Peereboom, D.M., Thorsheim, H.R., Samala, R., Balyan, R., Murphy, C.G., Lockman, P.R., Simmons, A., Weil, R.J., Tabar, V., and Steeg, P.S. (2014). Capecitabine and lapatinib uptake in surgically resected brain metastases from metastatic breast cancer patients: a prospective study. *Neuro-oncology*. 17, 289-295.

91. Sysa-Shah, P., Tocchetti, C.G., Gupta, M., Rainer, P.P., Shen, X., Kang, B.H., Belmonte, F., Li, J., Xu, Y., Guo, X., and Bedja, D. (2015). Bidirectional cross-regulation between ErbB2 and β -adrenergic signalling pathways. *Cardiovascular research*. 109, 358-373.
92. Kedrin, D., Wyckoff, J., Boimel, P.J., Coniglio, S.J., Hynes, N.E., Arteaga, C.L., and Segall, J.E. (2009). ERBB1 and ERBB2 have distinct functions in tumor cell invasion and intravasation. *Clinical Cancer Research*. 15, 3733-3739.

Figures legends

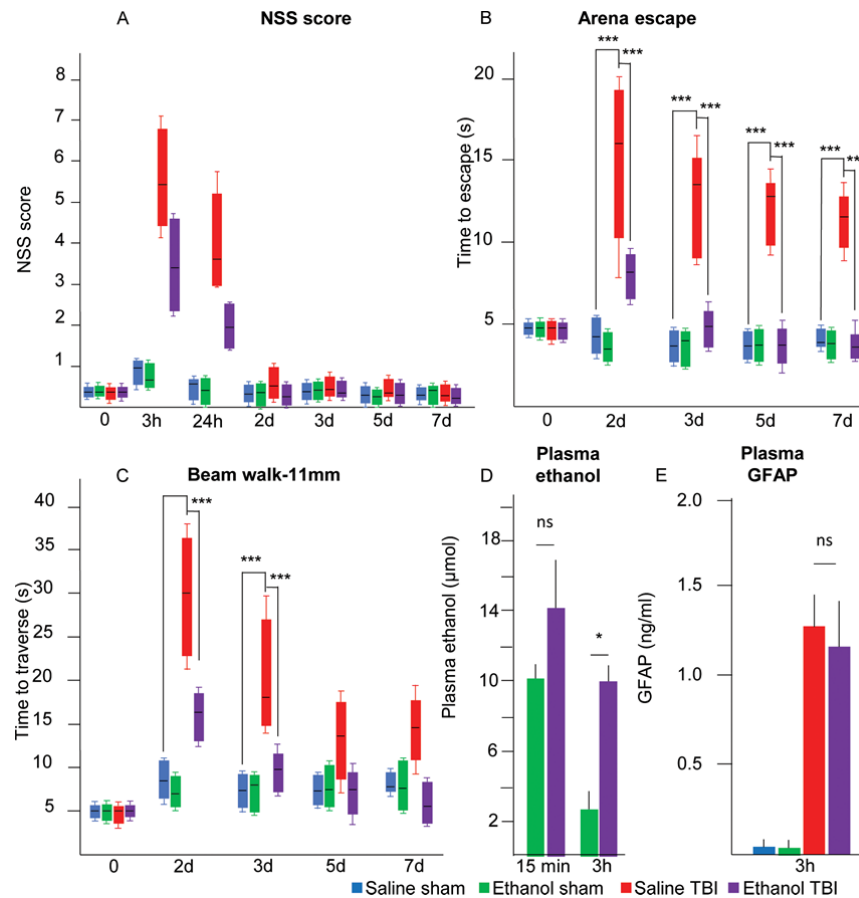


Figure 1. Neurological recovery after administration of Ethanol in TBI. A) The NSS score was higher after TBI compared to the sham controls but did not differ between ethanol and saline-pretreated mice. At 3h after injury, the NSS score was comparable in sal-TBI (n=8), eth-TBI (n=6) mice ($p=0.12$) and higher than in sal-S (n=3) or eth-S mice (n=3). Sal-TBI and eth-TBI mice displayed a progressive recovery in NSS score with eth-TBI displaying a trend towards faster neurological recovery ($p=0.55$). B) High-dose-ethanol-pretreated mice performed significantly better in the Arena Escape test. Sal-TBI (n=8) mice required significantly longer to exit arena than sal-S (n=3) or eth-S (n=3) controls ($p=0.0036$). Eth-TBI mice (n=6) were significantly faster at 2 dpi ($p=0.045$ vs sal-TBI, $p=0.75$ vs sham). The performance of sal-TBI mice did not improve with time ($p<0.001$ when compared to sal-S). C) High-dose ethanol-pretreated mice displayed a better performance in the Beam Walk test. Sal-TBI mice (n=8) performed worse than the sham controls ($p<0.0001$) with

progressive recovery of performance ($p=0.682$). Eth-TBI mice ($n=6$) performed significantly better than sal-TBI ($p<0.0001$) and recovered to baseline values within a shorter time interval (eth-TBI vs eth-S $p=0.78$; sal-TBI vs sal-S $p<0.001$). D) Ethanol pretreatment (5g/kg) resulted in a significant elevation in blood ethanol levels at 15min and 3h after trauma. At 15min, eth-S ($n=3$) and eth-TBI ($n=4$) mice display high levels of blood ethanol ($p=0.057$). At 3h blood ethanol levels were significantly lower in both groups, but the decline in eth-S ($n=3$) was significantly larger than in the eth-TBI ($n=4$) ($p<0.01$). E) Ethanol pretreatment does not affect blood GFAP levels after TBI. At the 3h time point, blood GFAP levels were comparable in sal-TBI ($n=4$) and in eth-TBI ($n=4$; $p>0.05$), as significantly higher than in sal-S ($n=3$) and eth-S ($n=3$) groups ($p<0.01$), respectively. Statistical analysis by two-way ANOVA with Tuckey post-hoc test.

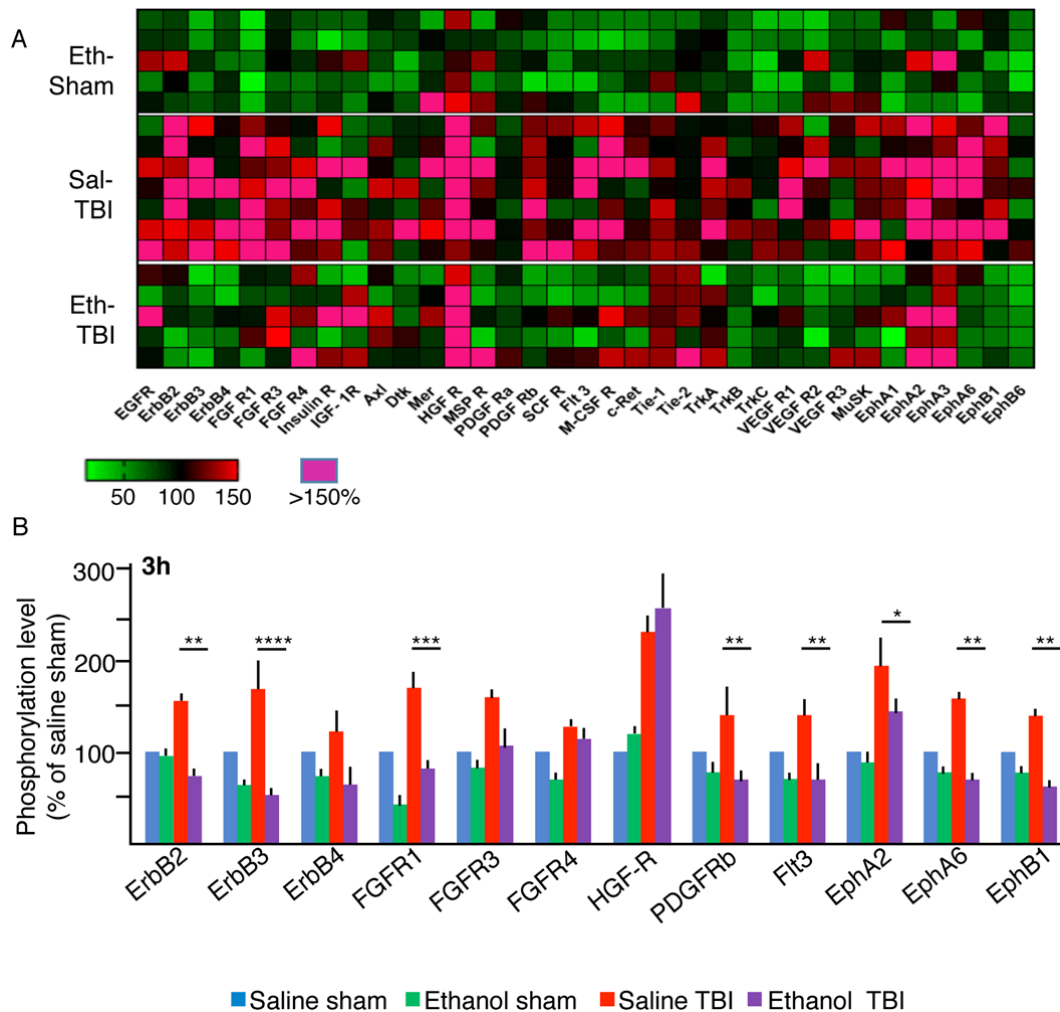


Figure 2. Phosphorylation of multiple RTKs after TBI and their modulation by Ethanol. A)

The heat map depicts the relative phosphorylation level of 38 RTK measured in samples from eth-S (n=5), sal-TBI (n=7) and eth-TBI (n=5), using sal-S (n=8) as baseline. TBI induces a significant increase in phosphorylation of 11 RTKs (ErbB2, ErbB3, FRFG1, FGFR3, FGFR4, HGF-R/c-Met, PDGFR- β , Flt3, EphA2, EphA6 and EphB1) at the 3h time point. Ethanol pretreatment decreases the phosphorylation of ErbB2, ErbB3, FGFR1, PDGFR β , flt3, EphA6 and EphB1 but not of FGFR2 and 3, HGFR and EphA6. B) Quantification of a subset of RTK phosphorylation after TBI. In whole-cortex protein extract, TBI upregulates ErbB2, ErbB3 and FGFR1 whereas, ethanol pretreatment prevents the upregulation (ErbB2: p=0.0003; ErbB3: p<0.0001; FGFR1: p=0.001; Flt3: p=0.0088; EphA6: p=0.0011; EphB1 p=0.0041). Statistical analysis by two-way ANOVA with Tuckey post-hoc test. For clarity only statistical significance for comparisons between sal-TBI and eth-TBI are graphically depicted.

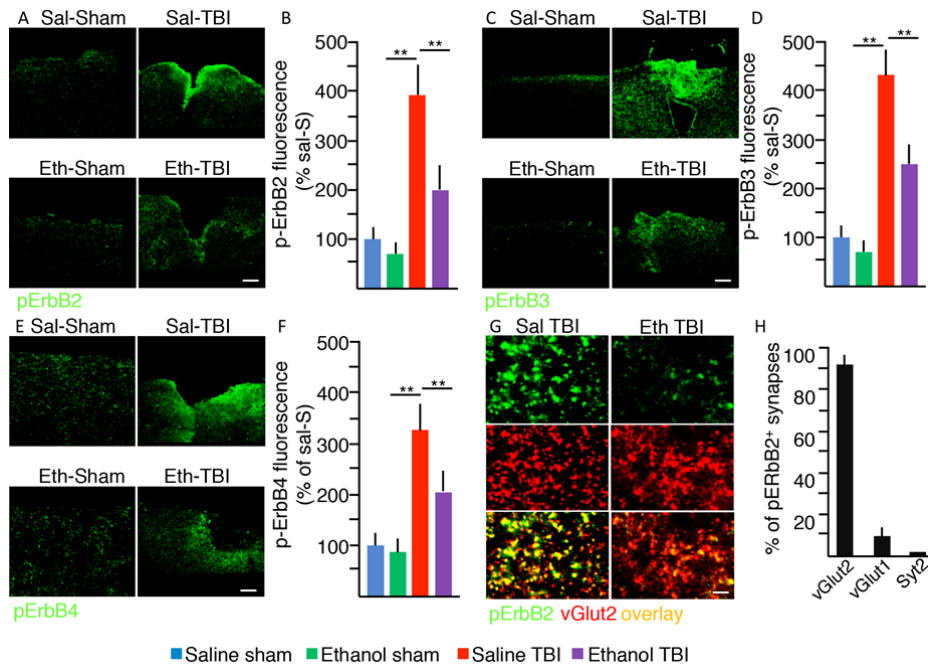
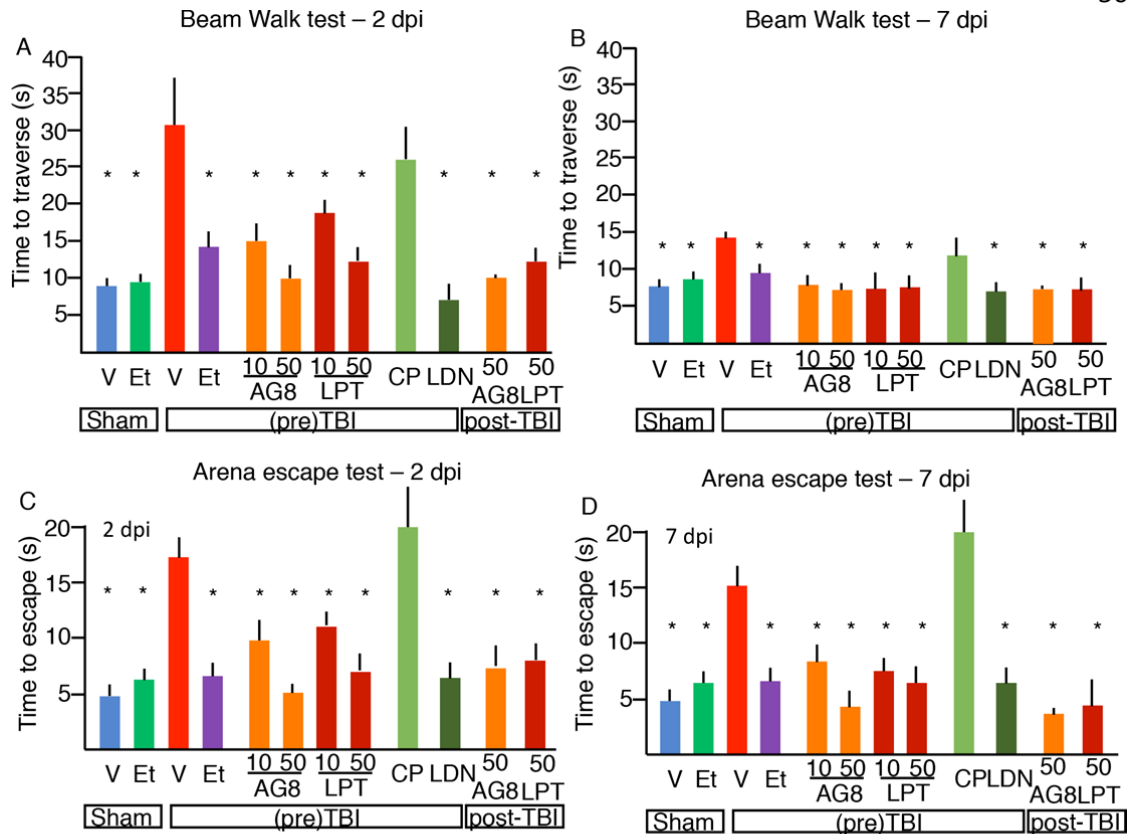


Figure 3. Suppression of TBI-induced phosphorylation of ErbB2 and ErbB3 in vGlut2⁺ excitatory synapses by Ethanol.

A-B) Levels of phosphorylated ERbB2 were increased 3h after TBI. Immunofluorescence intensity for pErbB2 was increased to $371 \pm 68\%$ of sal-S ($n=4$; $p < 0.01$) in sal-TBI mice ($n=5$), whereas ethanol pretreatment resulted in the reduced elevation of pERbB2 levels ($n=4$; $p < 0.01$ vs sal-TBI and vs sal-S and eth-S) after TBI (eth-TBI). Scale bar $50 \mu\text{m}$. C-D) Levels of phosphorylated ErbB3 were increased after TBI. Immunofluorescence intensity for pErbB3 significantly increased compared to sal-S ($p < 0.01$) at 3h in sal-TBI mice ($n=4$), whereas ethanol pretreatment (eth-TBI, $n=4$) resulted in reduced elevation of pERbB2 levels ($p < 0.01$ vs sal-TBI and vs sal-S) after TBI. Scale bar $50 \mu\text{m}$. E-F) Increased levels of phosphorylated ErbB4 was noted after TBI. Immunofluorescence intensity for pErbB4 was significantly increased ($n=4$; $p < 0.01$) at 3h in sal-TBI mice, whereas ethanol pretreatment results in the reduced elevation of pERbB4 levels ($n=4$; $p < 0.01$ vs sal-TBI and vs sham) after TBI. Scale bar $50 \mu\text{m}$. G-H) ERbB2 phosphorylated at vGlut2⁺ synapses after TBI. At 3h post injury (sal-TBI; $n=3$), $93 \pm 4\%$ of pErbB2 clusters co-localized with vGlut2 whereas only $3 \pm 2\%$ co-localized with vGlut1 and never with inhibitory synapses synaptotagmin-2⁺. Statistical analysis by two-way ANOVA. Scale bar $2 \mu\text{m}$.



Chandrasekar.Fig4

Figure 4. Improvement in behavioral outcome by administration of ErbB inhibitors before or after TBI.

A, B) Treatment with ErbB inhibitor AG825 or Lapatinib before or after TBI resulted in improved recovery in the Beam Walk test. To demonstrate whether, selective RTK inhibition may recapitulate EI effect, mice were administered with either 10mg/kg or 50mg/kg of the ErbB2-specific inhibitor Lapatinib (n=6 and n=4, respectively) or of the pan-ErbB inhibitor AG825 (n=5 and n=4, respectively) 30min before TBI. Mice treated with the 10 mg/kg of AG825 or Lapatinib performed significantly better than vehicle-treated TBI mice at 2 dpi; $p < 0.001$ vs veh-TBI for both compounds). Mice administered with 50mg/kg AG825 or Lapatinib mice showed a trend towards better performance than the mice administered with 10mg/kg dose ($p < 0.05$ for Lapatinib 10mg vs 50mg). Administration of the broad-selectivity RTK inhibitor LDN-211904 (10mg/kg; n=4) also produced a significant improvement in performance ($p < 0.01$ vs veh-TBI) whereas the PDGFR-selective drug CP-

673451 (10mg/kg, n=4) did not affect significantly the performance ($p>0.05$ vs veh-TBI). Administration of AG825 or Lapatinib (50mg/kg; n=4 and n=4, respectively) 30min after TBI resulted in a significant improvement in performance at 2 dpi ($p<0.05$ vs veh-TBI). At 7 dpi, eth-TBI as well as mice treated with either dose of Lapatinib, AG825 or LDN were similar in performance to sal-S or eth-S mice, whereas sal-TBI were still significantly slower. Statistical analysis by one-way ANOVA with Bonferroni post-hoc test. C, D) Performance in the Arena Escape test was significantly improved in mice pretreated with AG825 (10mg/kg or 50mg/kg, n=5 and n=4, respectively), Lapatinib (10mg/kg or 50mg/kg, n=6 and n=4, respectively) or LDN-211904 (10mg/kg, n=4). At 2 dpi, AG825, Lapatinib, 10 or 50mg/kg and LDN-211904-pretreated mice performed significantly better than veh-TBI mice ($p<0.05$). Mice pretreated with the PDGFR inhibitor (10mg/kg, n=3) performed comparable to the veh-TBI mice. At 7 dpi, mice treated with ethanol, Lapatinib, AG825 or LDN-211904 displayed a comparable performance and were significantly better than vehicle-treated TBI mice. Notably, mice treated with either 50mg/kg AG825 or 50mg/kg Lapatinib (n=4 and n=4, respectively) 30min after TBI displayed a significant improvement in performance compared to sal-TBI ($p<0.05$). This beneficial effect was persistent at 7 dpi. Statistical analysis by one-way ANOVA with Bonferroni post-hoc test. For clarity, statistical significance indicated graphically is corresponding to the comparison each treatment group with veh-TBI.

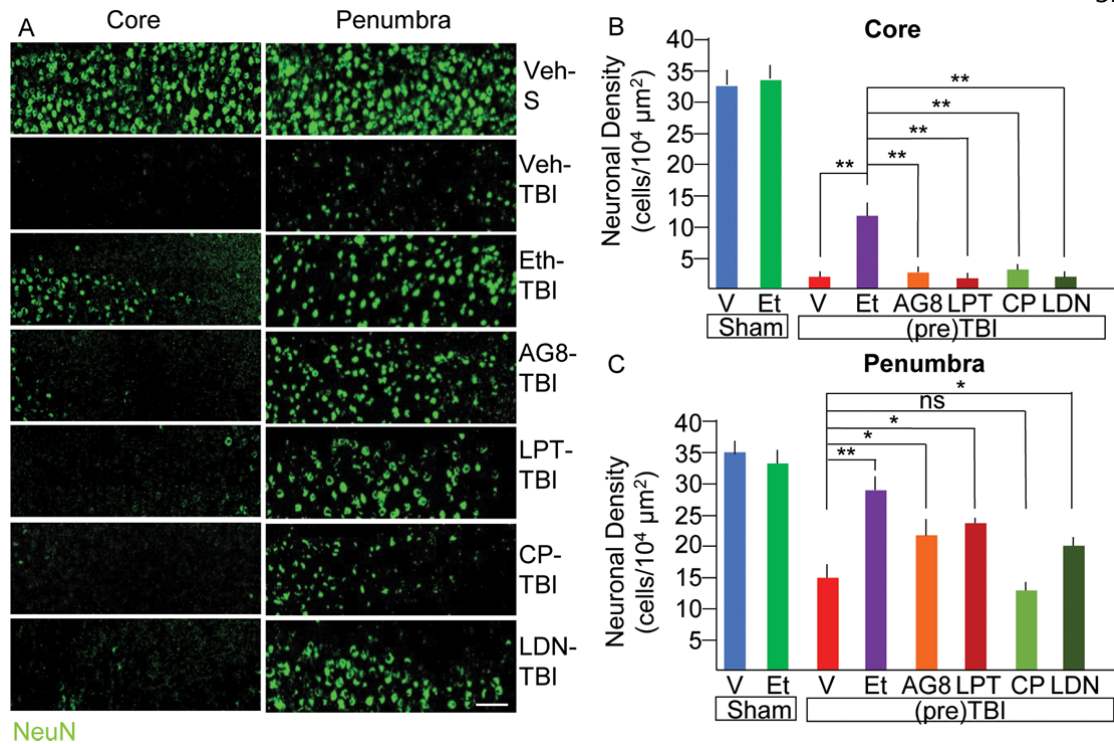


Figure 5. Ethanol pretreatment and ErbB inhibitors treatment reduces neuronal loss after TBI.

A-C) At 7 dpi, mice administered with vehicle alone (n=3) or ethanol (n=3) in vehicle which underwent sham surgery displayed a comparable density of NeuN⁺ cells in the “core” and in the “penumbra” ROI. Veh-TBI (n=6) displayed an almost complete loss of NeuN⁺ cells in the core as compared to veh-S (p<0.001) and a significant decrease of NeuN⁺ in penumbra (p<0.001). Ethanol pretreatment (eth-TBI; n=4) resulted in a larger population of NeuN⁺ cells at the injury site (p<0.01) and in the penumbra (p<0.01; vs both veh-S and veh-TBI). Administration of ErbB inhibitors (10mg/kg; n=6 and n=5 for Lapatinib and AG825) or of broad-spectrum RTK inhibitor LDN-211904 (10mg/kg, n=4) did not affect NeuN⁺ cells in the core (p>0.05 vs veh-TBI), but significantly preserved it in the penumbra (as compared to veh-TBI, p<0.05). Administration of the PDGFR inhibitor (10mg/kg; n=4) did not affect the number of NeuN⁺ cells in the core (p>0.05) or in the penumbra (p>0.05). Statistical analysis by one-way ANOVA with Bonferroni post-hoc test. Scale bar 20μm.

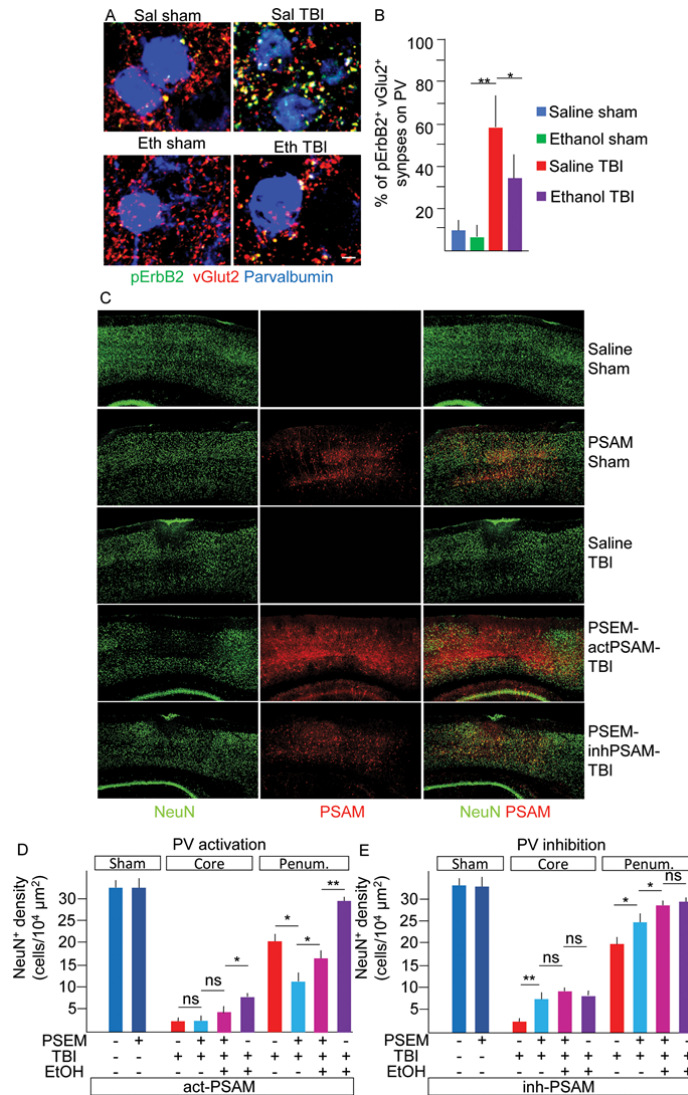


Figure 6. pErbB phosphorylation involves excitatory synapses on PV interneurons and chemogenetic suppression of PV interneurons reduces neuronal loss after TBI.

A, B) pErbB activation in excitatory synapses on PV interneurons is reduced by ethanol pretreatment. In sal-TBI mice a significantly larger fraction of vGlut2⁺ synapses was pErbB2⁺ compared to sal-S and eth-S; in eth-TBI samples, however, the fraction of vGlut2⁺ ErbB2⁺ synapses on PV interneurons were significantly lower than in sal-TBI samples (p<0.05 sal-TBI vs eth-TBI). Scale bar 4μm. C-E) Enhancement of PV interneuron activity reduced neuronal survival. All PV-Cre mice were injected with the AAV9 for PSAM expression. In sham-operated mice (sal-actPSAM-S n=3, PSEM-actPSAM-S n=3; sal-inhPSAM-S n=3, PSEM-inhPSAM-S n=3, n=3), NeuN⁺ cells counts were comparable at 7 dpi

($p > 0.05$; panel C-E) and were comparable to saline-treated, naïve mice (panel C). Sal-TBI (sal-actPSAM-TBI $n=4$; sal-inhPSAM-TBI $n=4$) resulted in the almost complete loss of NeuN⁺ cells in the core lesion ($p < 0.05$ vs sham samples) and a significant decrease in the penumbra ($p < 0.05$). Activation of PV interneurons firing (PSEM-actPSAM-TBI; $n=5$) did not affect the number of NeuN⁺ cells in the core (panel D), but worsened the loss of NeuN⁺ immunoreactivity in the penumbra ($p < 0.05$ vs sal-actPSAM-TBI; panel D). Conversely, inhibiting PV interneurons (PSEM-inhPSAM-TBI; $n=5$) resulted in higher number of NeuN⁺ cells in the core (panel E) and significantly higher NeuN⁺ cells in the penumbra ($p < 0.05$ vs sal-inhPSAM-TBI; panel E). Co-administration of ethanol and PV inhibition (eth-PSEM-inhPSAM-TBI; $n=4$) did not increase neuronal survival further in the core lesion ($p > 0.05$ vs PSEM alone; panel E), but further enhanced the preservation of neurons in the penumbra ($p < 0.05$ vs sal-actPSAM-TBI and vs PSEM-inhPSAM-TBI; panel E) to a level comparable to eth-inhPSAM-TBI mice ($n=3$). Reciprocally, application of ethanol together with PV activation (eth-PSEM-actPSAM-TBI, $n=4$) did not increase the number of NeuN in the core but increases neuronal preservation in the penumbra ($p < 0.05$ vs PSEM-actPSAM-TBI; panel D), while both values remain lower than eth-actPSAM-TBI mice ($n=3$). Statistical analysis by one-way ANOVA with Bonferroni post-hoc test. Scale bar 200 μ m.

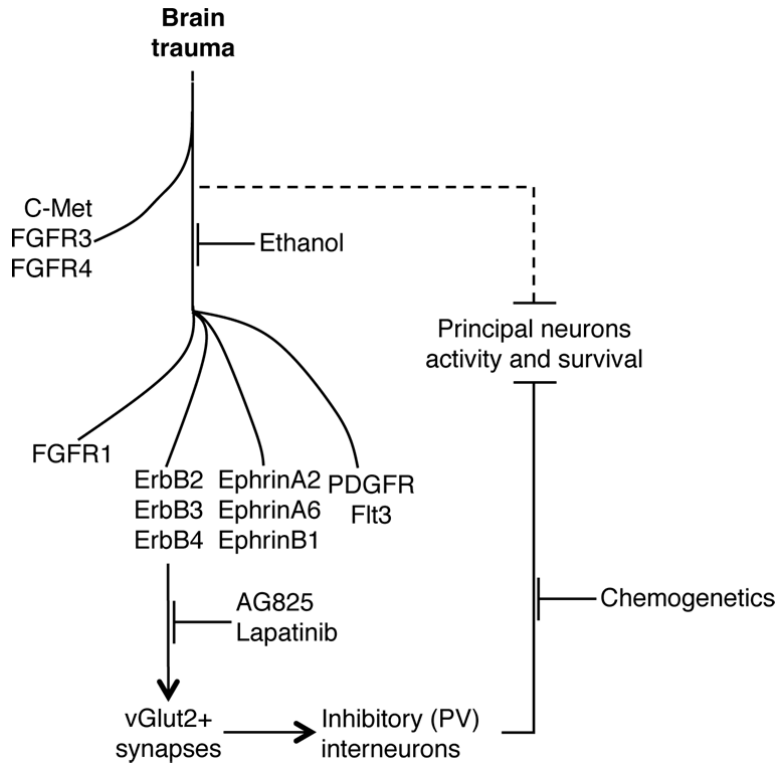


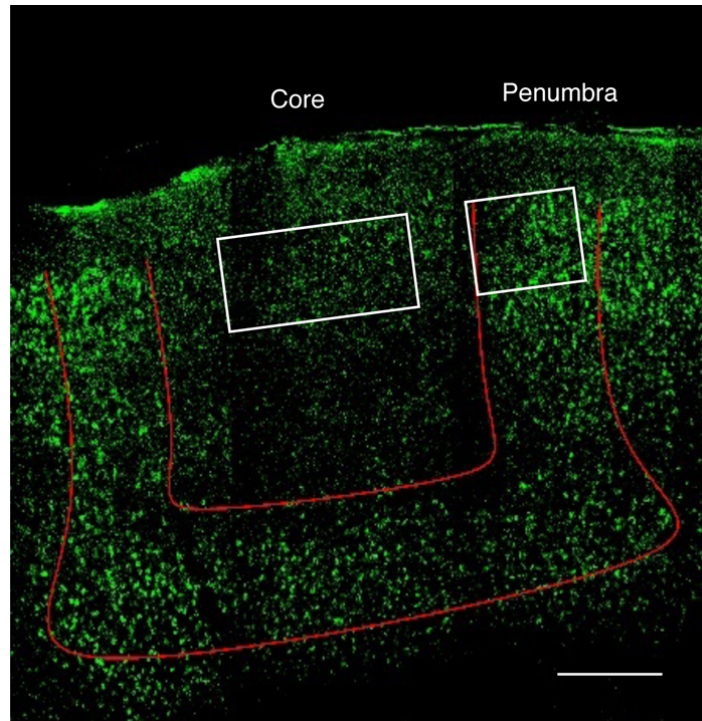
Figure 7. ErbB-mediated effect of ethanol on inhibitory microcircuitry after TBI. Ethanol pretreatment results in the suppression of the activation of multiple RTKs by TBI. In particular, TBI-induced activation of ErbB phosphorylation in vGlut2+ synapses on PV interneurons is suppressed by ethanol. Loss of excitation due to excess inhibition may increase the vulnerability of neurons to TBI-induced neurotoxic cascades and by suppressing PV-mediated perisomatic inhibition, ethanol may enhance neuronal survival. This effect is recapitulated by either direct ErbB inhibition or by direct suppression of PV firing by chemogenetics.

Supplementary table1. Number of mice used in each treatment group according to the experimental design.

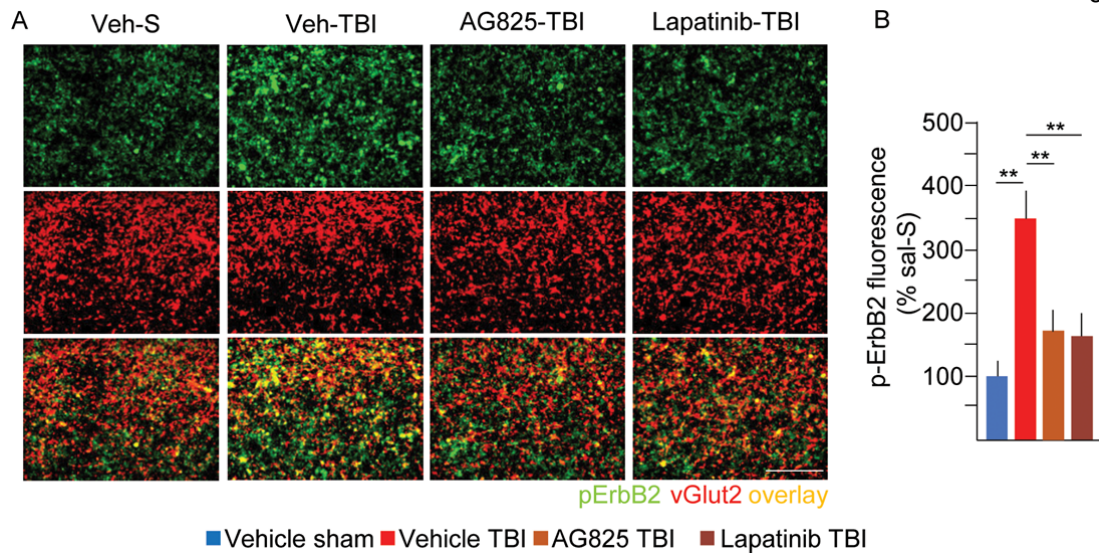
Experimental goal	Treatment groups	Number of mice	readout	total	
Behavioral performance	Sal-S	3	NSS, Arena	20	
	Eth-S	3	Escape, Beam		
	Sal-TBI	8	Walk, Open		
	Eth-TBI	6	Field; NeuN+ cells at 7 days		
RTK array	Sal-S	8	RTK phosphorylation at 3h after TBI (or Sham surgery)	25	
	Eth-S	5			
	Sal-TBI	7			
	Eth-TBI	5			
Blood gas and blood ethanol levels 15 min after TBI	Sal-S	3	paO ₂ , paCO ₂ , Blood ethanol level	13	
	Eth-S	3			
	Sal-TBI	4			
	Eth-TBI	3			
Blood ethanol levels and blood GFAP levels 3h after TBI	Sal-S	3	Blood ethanol level; blood GFAP levels	14	
	Eth-S	3			
	Sal-TBI	4			
	Eth-TBI	4			
Phosphorylated ErbB histology	Sal-S	3	Immunostaining for phospho-ErbB2, phospho-ErbB3, phospho-ErbB4	15	
	Eth-S	3			
	Sal-TBI	5			
	Eth-TBI	4			
Effect of specific ErbB or RTK inhibitors	Sal-S	4	NSS, Arena		
	Eth-S	3			Escape, Beam
	Sal-TBI	5			Walk, Open

	Eth-TBI	4	Field; NeuN+ cells at 7 days	51
	Pret. Lapatinib 10mg/kg	6		
	Pret. Lapatinib 50mg/kg	4		
	Pret. AG825 10mg/kg	5		
	Pret. AG825 50mg/kg	4		
	Pret. LDN	4		
	Pre. CP	4		
	Post Lapatinib 50 mg/kg	4		
	Post AG 825 50 mg/kg	4		
	Effect of ErbB inhibitors on ErbB phosphorylation 3h after TBI	Sal-S		
Sal-TBI		3		
Pret. AG825 50mg/kg		3		
Pret. Lapatinib 50 mg/kg		3		
Chemogenetics	Sal-actPSAM-S	3	NeuN+ cells count at 7 days	
	Sal-inhPSAM-S	3		
	PSEM-actPSAM-S	3		
	PSEM-inhPSAM-S	3		
	Sal-actPSAM-TBI	4		
	Sal-inhPSAM-TBI	4		
	PSEM-actPSAM-TBI	5		
	PSEM-inhPSAM-TBI	5		
	Eth-actPSAM-TBI	3		
	Eth-inhPSAM-TBI	3		
	Eth-PSEM-actPSAM-TBI	4		
	Eth-PSEM-inhPSAM-TBI	4		

				58
				44
Total number of mice used				194



Supplementary Figure 1. Position of “Core” and “Penumbra” ROI for neuronal survival assessment. NeuN⁺ cells density was evaluated in two ROIs. One is located in the core of the TBI lesion (on the axis of the lesion) and one at a fixed distance (penumbra). Scalebar 200 μ m.



Supplementary Figure 2. Administration of ErbB specific inhibitors decreases TBI-induced phosphorylation of ErbB2.

A-B) Phosphorylation levels of pErbB2, assessed by immunofluorescence intensity, were increased 3h after TBI to $354 \pm 60\%$ of sal-S ($n=3$; $p < 0.01$). Pre-treatment with 50mg/kg ErbB inhibitors AG825 and Lapatinib significantly reduced the phosphorylation of ErbB2 after TBI to $162 \pm 46\%$ (AG825 vs TBI, $p < 0.01$; $n=3$) and $153 \pm 65\%$ (Lapatinib vs TBI, $p < 0.01$; $n=3$). Statistical analysis by two-way ANOVA. Scalebar 20 μ m.